CHARACTERISTICS AND APPLICATIONS OF PLASMONIC MATERIALS ALTERNATIVE TO GOLD AND SILVER

by

Rafiuddin Alvi —----------------- 170021102
Toukir Shahriair —--------------- 170021103
Abdelrahman Shohdy —------ 170021179

A Thesis Submitted to the Academic Faculty in Partial Fulfillment of the Requirements for the Degree of

BACHELOR OF SCIENCE IN
ELECTRICAL AND ELECTRONIC ENGINEERING

Department of Electrical and Electronic Engineering
Islamic University of Technology (IUT)
Gazipur, Bangladesh

May 2022

CHARACTERISTICS AND APPLICATIONS OF PLASMONIC MATERIALS ALTERNATIVE TO GOLD AND SILVER

Approved by:

____

Mr. Md. Omar Faruque

Supervisor and Assistant Professor,
Department of Electrical and Electronic Engineering
Islamic University of Technology (IUT)
Gazipur, Bangladesh

Date: 17.05.2022

Toukir Shahriair

Toukir Shahriair
170021103

Rafiuddin Alvi
170021102

Abdo

Abdelrahman Shohdy
170021179

Table of Contents

Acknowledgement

We express our gratitude to Allah from the bottom of our hearts as we were able to conduct this research properly and complete our thesis because He enabled us to do so. Also, we want to thank our respected supervisor, **Mr. Md. Omar Faruque**, for his guidance and help. Without his help and support, we would not be able to complete our research in a proper way.

We would also like to thank all the EEE Dept faculty members, IUT for their support. They gave us the proper environment for us to learn and do our research in a constructive way.

And last, we would like to give our deepest gratitude to our family members. They always were by our sides during our sufferings and also motivated us to properly conduct the research.

Abstract

In our modern world, plasmonic materials are used in many scientific sectors. They are mostly used in chemical sensing, information processing, further size reductions, miniaturize optical components etc. Gold and silver are the conventional materials used in plasmonic materials. But these materials also have some problems regarding their characteristics. There are some unconventional materials that show similar characteristics. The real as well as the imaginary parts of the refractive index of these atypical materials employed in the doping element in the proposed model of COMSOL simulations can be obtained using the Lorentz-Drude model. From the simulations, transmittance vs wavelength graphs are generated which are compared to the outputs of gold and silver. A comparative analysis is included for a better insight.

Chapter 1

Introduction

1.1 Overview

Novel applications are enabled by materials technology, which aids in the discovery of new research.This is the result of advancement in materials technology. Materials are crucial in the positive feedback loop that has been built between research and technology. Semiconductor technologies and optical communications are two of the most common examples from the previous century. Ability to process data, and the speeds at which we can process data have increased exponentially in recent decades by these fields, owing to Moore's Law's expected scaling of semiconductor electronic components. However, significant scaling creates numerous challenges, including short-channel effects, gate leakage, and dramatically increased power density. Alternative technologies have gotten a lot of attention as a result of these issues in the effort to boost information processing rates. Plasmonics is one such alternative technology that has the ability to meet our ever-increasing information processing needs. We examine recent discoveries in the emerging field of plasmonics materials research. This research focuses on the design of metal-like materials employing atypical materials, and addresses their benefits and drawbacks in various plasmonics and metamaterials applications.

1.2 Research Objective

In plasmonic and optical metamaterial systems, gold and silver are commonly employed. However, there are certain unusual materials that have essentially identical qualities. The goal of this study is to develop a superior plasmonic material for turning groundbreaking scientific discoveries into next-generation technology.

1.3 Thesis Outline

This thesis work proposes a replacement for conventional plasmonic materials. Mostly gold and silver are used as plasmonic materials. But there are other materials that can replace gold and silver. We run simulations of various materials and choose the best replacement among them.

In chapter 2, we gave some theoretical information about plasmonic materials. We talked about the applications of these plasmonic materials. We also talked about the advantages and disadvantages of using conventional plasmonic materials.

In chapter 3, we discussed the mathematical model and design. We used the Lorentz-Drude model to characterize the frequency dependent complicated dielectric permittivity of strongly doped materials. We also gave a figure which shows the model that was used on simulation.

In chapter 4, we gave the simulation outputs and results. We generated electric fields(EWFD) as well as transmittance vs wavelength graphs for different materials.

Chapter 5 includes the comparison of outputs. We compared the results of different materials with gold and silver in order to find out which material will be best to replace them.

Chapter 2

Theoretical Background

2.1 Plasmonic Materials

Despite the fact that some plasmonic applications have been known for a long time, plasmonics has recently attracted a lot of attention. The metal's free electrons can generate charge density on the metal's surface when light interacts with it. Surface plasmon waves are a phenomenon that can be used in many advanced applications. Surface plasmons can firmly bind light to the surface of metal, enhancing light-matter interactions significantly. Scaling nanoelectronic components is difficult, there is an increasing desire for new technologies that enable quicker processing rates. Optical transmission is the fastest available mode of information processing due to its extremely wide bandwidth. Optical components, on the other hand, are bulky and can't be packed as densely as nanoelectronic components. Each integrated circuit chip, for example, is made up of billions of nanometer-sized transistors. Optical components can not have high density packing due to diffraction limit. Optical systems that are traditionally used can only focus light to a size on the order of the wavelength due to diffraction effects. To avoid diffraction, optical components should be a few hundreds of nanometers in size. To get the requisite optical properties of a metamaterial, meta-molecules must be properly developed. New functions including optical magnetism, sub-diffraction resolution, and a negative refractive index have been shown using metamaterials and TO principles. The real part represents the polarization response, whereas the imaginary part represents the losses produced by optics. Metals have a negative real permittivity at different optical frequencies, whereas dielectrics have a positive real permittivity. The imaginary part of the permittivity can be minimal in dielectrics, but not in metals, which are usually associated with losses owing to electronic transitions. Loss drastically limits the performance of optical equipment. Metal problems stymie the design, manufacture, and integration of different plasmonic and metamaterial devices.. The next section provides a summary of the major issues that typical plasmonic materials have.

2.2 Applications of Plasmonic Materials

2.2.1 Chemical Sensing

Chemical sensing is a huge part in the applications of plasmonic materials. plasmonics increases light-matter interactions by small changes in the local environment that can be amplified dramatically, allowing for ultrasensitive detection.

2.2.2 Information Processing

Information processing is another key potential application of plasmonics. Because scaling nanoelectronic components is difficult, new technologies are needed to enable faster processing speeds. Because of its incredibly large bandwidth, optical transmission is the quickest available method of information processing.

2.2.3 Further Size Reductions

Optical components are larger than nanoelectronic components and cannot be packed as securely. Each integrated circuit chip, for example, is made up of billions of nanometer-sized transistors. Such high-density packing is not possible for optical components due to the diffraction limit. Optical systems that are traditionally used can only focus light to a size on the order of the wavelength due to diffraction effects. Optical components should be at least a few hundreds of nanometers in size to avoid diffraction. Plasmonics enables for much smaller size reductions than diffraction allows.

2.2.4 Miniaturize Optical Components

We can miniaturize optical components and integrate them on-chip using plasmonics while exploiting light's enormous bandwidth.

2.3 Advantages of Gold and Silver

Silver as well as gold are frequently used in plasmonic systems due to their low ohmic loss property and excellent DC conductivity. Metallic properties in these metals aid the performance of the device, flexibility in design also fabrication, integration, and tunability.

2.4 Problems with Conventional Plasmonic Materials

At optical wavelengths, however, a loss mechanism known as interband transitions plays a key role in gold and silver. When a valence electron in a metal absorbs a photon to jump to the Fermi surface, or when an electron at the Fermi surface absorbs a photon to jump to the next vacant conduction band, Interband transitions occur. This is the process by which copper and gold lose their color. There are two types of interband and intraband losses expressed by the imaginary fraction of permittivity. In the near-infrared (NIR), gold has substantial intraband losses (or Drude losses) and smaller intraband losses (or Drude losses) at shorter wavelengths. For shorter wavelengths in the visual range, however, interband losses in gold are significant. Interband transitions provide additional losses at optical frequencies, rendering conventional metals unsuitable for many plasmonic and metamaterial systems.

Chapter 3

Theoretical Method and Device Design

3.1 Mathematical Model

The Lorentz-Drude model can be used to characterize the frequency-dependent complicated dielectric permittivity of strongly doped materials.

$$\varepsilon(\omega) = \varepsilon_\infty - \frac{\omega_p^2}{\omega^2\left(1 + i\frac{1}{\omega\tau}\right)}$$

Separating the real and imaginary part,

$$\varepsilon(\omega) = \left(\varepsilon_\infty - \frac{\omega_p^2\tau^2}{1+\omega^2\tau^2}\right) + i\frac{\omega_p^2\tau}{\omega\left(1+\omega^2\tau^2\right)}$$

Usually, the angular frequency is greater than plasma frequency and electron/hole relaxation time is greater than 1. So, the equation can be written as,

$$\varepsilon(\omega) = \left(\varepsilon_\infty - \frac{\sigma}{\omega^2\varepsilon_0\tau}\right) + i\frac{\sigma}{\omega^3\tau^2\varepsilon_0}$$

The refractive index of a material can be calculated using an equation given below.

$$n \pm i\kappa = \sqrt{\varepsilon(\omega)}$$

3.2 Device Design

We designed a model in COMSOL software in order to run a simulation. The model is given below.

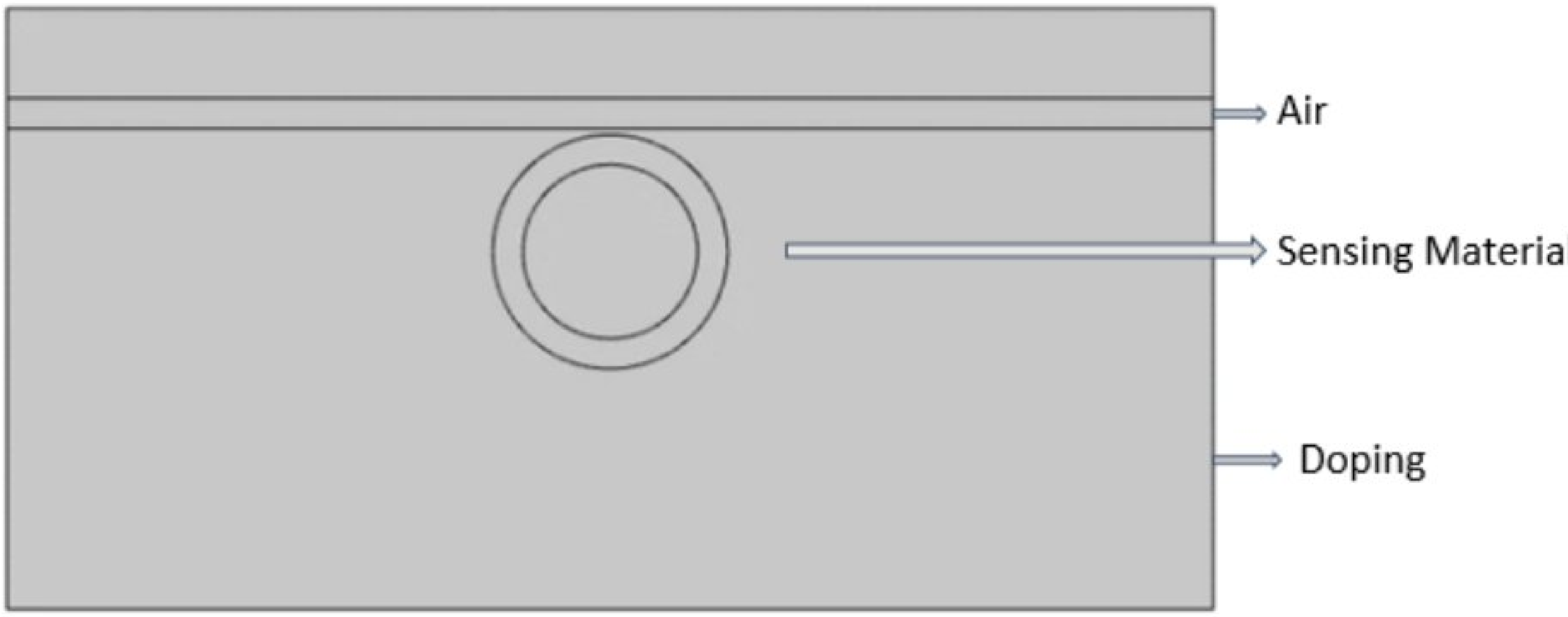

Figure 3.1 Model used for simulation

We changed the doping material and re-run the simulation to obtain graphs in order to compare with gold and silver. We used MATLAB coding to find out the real as well as imaginary parts of the refractive index of different materials. For this, we used a data table for the required equation.

Table 3.1 Data table for MATLAB Coding

Material	Background permittivity (ε_b)	Carrier mobility when heavily doped [$cm^2 V^{-1} s^{-1}$]	Effective mass (m^*)	Relaxation rate [eV]	Carrier concentration required to achieve Re{ ε } = − 1 at λ = 1.55 μm [$\times 10^{20} cm^{-3}$]	Im{ ε } or losses at λ = 1.55 μm
n-Si [4]	11.70	80 [14]	0.270	0.0536	16.0	0.8508
p-Si [5]	11.70	60 [14]	0.390	0.0495	23.1	0.7853
n-SiGe [6]	15.10	50 [15]	0.24	0.0965	18.2	1.9414
n-GaAs [7]	10.91	1000 [16]	0.068	0.017	3.76	0.2534
p-GaAs [8]	10.91	60	0.44 [17]	0.0438	24.4	0.6528
n-InP [9]	9.55	700	0.078	0.0212	3.82	0.2796
n-GaN [10]	5.04	50	0.24	0.0965	6.83	0.7283
p-GaN [10]	5.24	5	1.4	0.1654	42.3	1.290
Al:ZnO [11]	3.80	47.6	0.38	0.064	8.52	0.384
Ga:ZnO [12]	3.80	30.96	0.38	0.0984	8.59	0.5904
ITO [13]	3.80	36	0.38	0.0846	8.56	0.5077

Chapter 4

Simulations and Results

4.1 Reference Materials

4.1.1 Gold

The impact of varying structural parameters in the core, such as gold layer thickness, diameter of air hole, and varied forms of air holes, is also explored. The sensor described here could be a promising contender in the fields of detection of biological samples, sensing of organic chemical, and recognition of biomolecule.

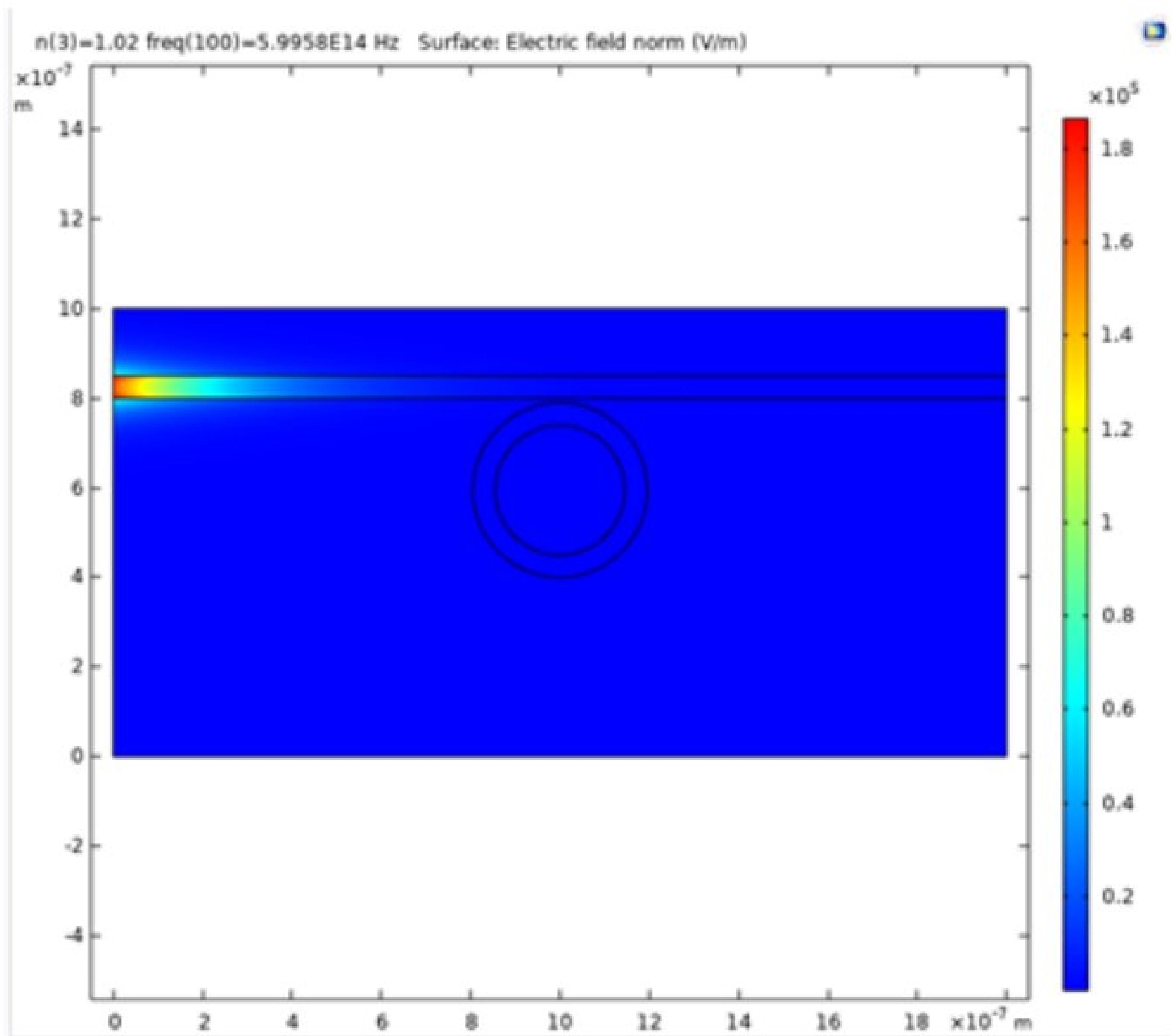

Figure 4.1 Electric Field(EWFD) of Gold

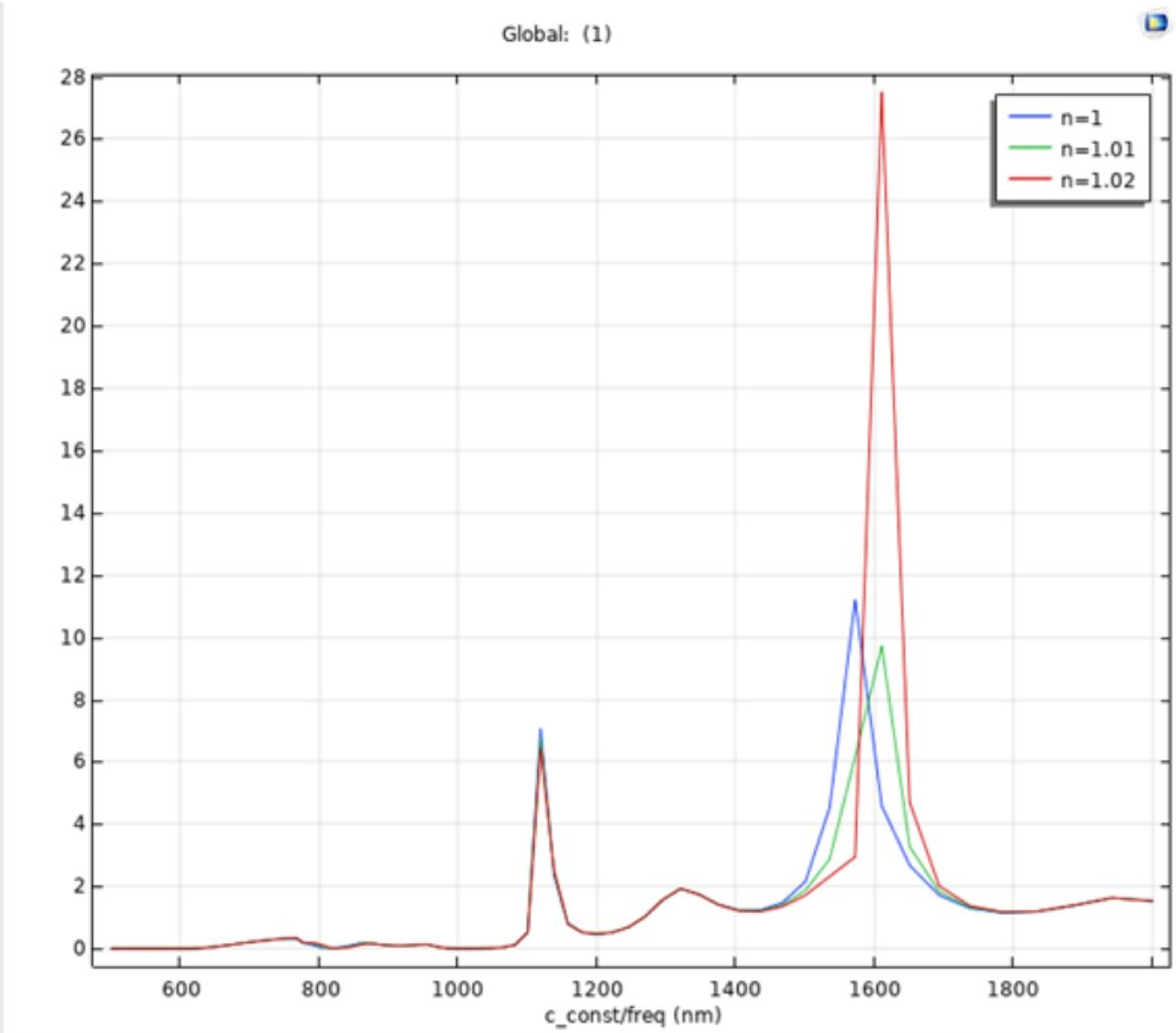

Figure 4.2 Transmittance vs Wavelength of Gold

4.1.2 Silver

Surface plasmons facilitate this connection, which is dependent on the form and arrangement of the nanocrystals. This assembly strategy provides a new, practical method for creating novel plasmonic materials for use in spectroscopic sensors, subwavelength optics, and integrated electronics that take advantage of field-enhancement phenomena.

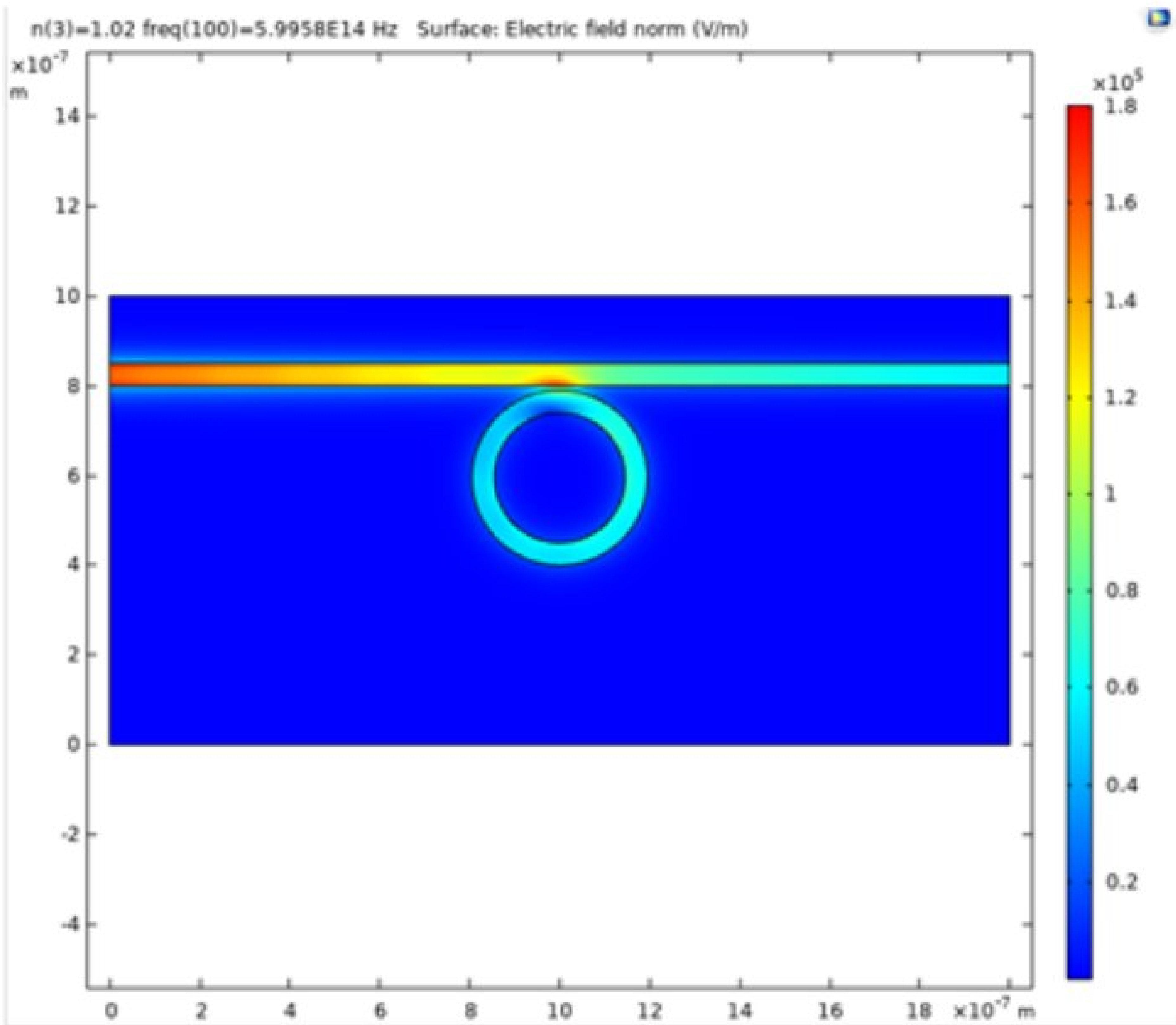

Figure 4.3 Electric Field(EWFD) of Silver

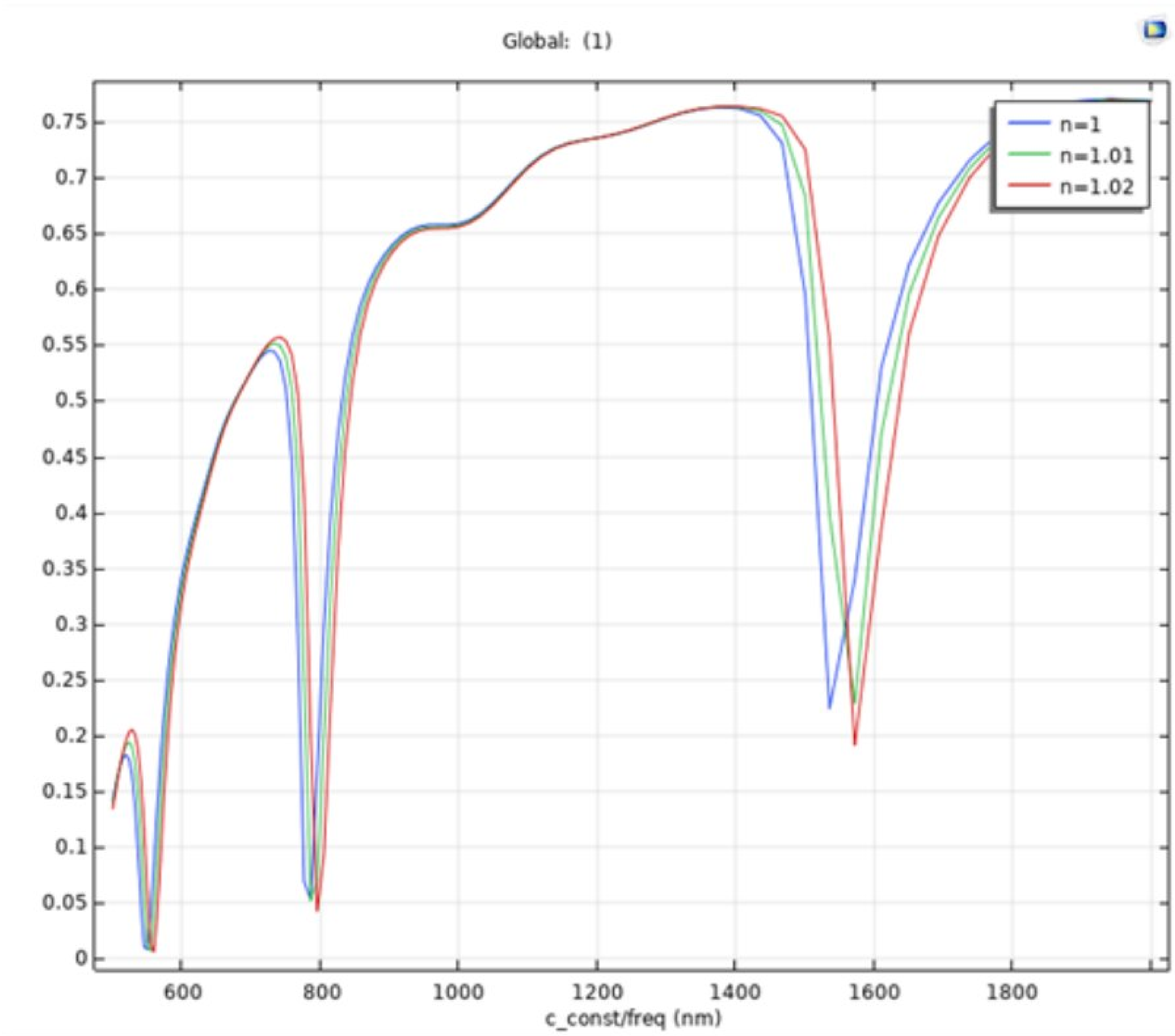

Figure 4.4 Transmittance vs Wavelength of Silver

4.2 Alternative Materials

4.2.1 n-Si

Group V elements can dope silicon in the n-type. Because electrons that work on the conduction in silicon have a substantially lower effective mass than holes, the plasma frequency for n-type silicon will be larger than for p-type silicon at the same doping amount.

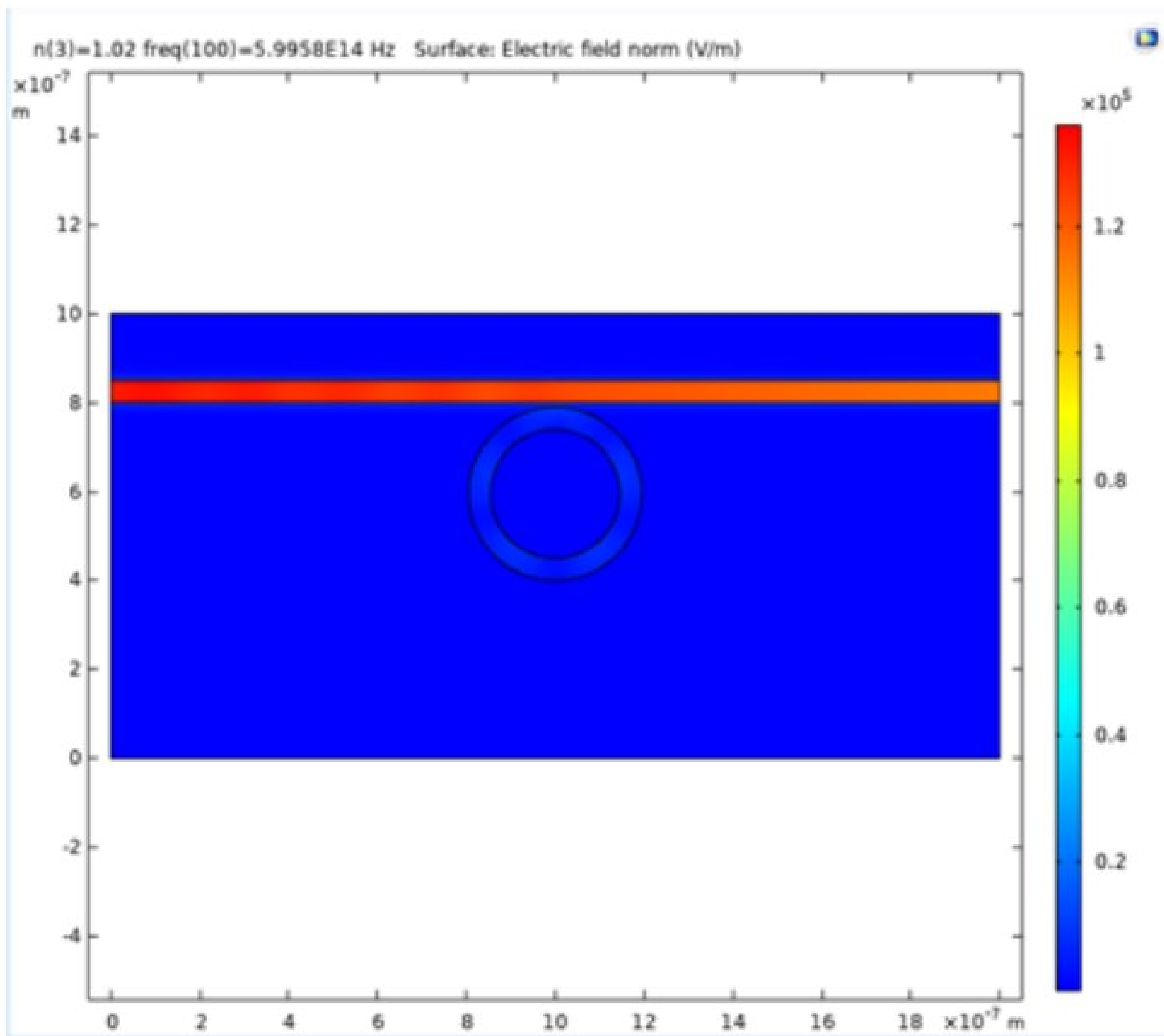

Figure 4.5 Electric Field(EWFD) of n-Si

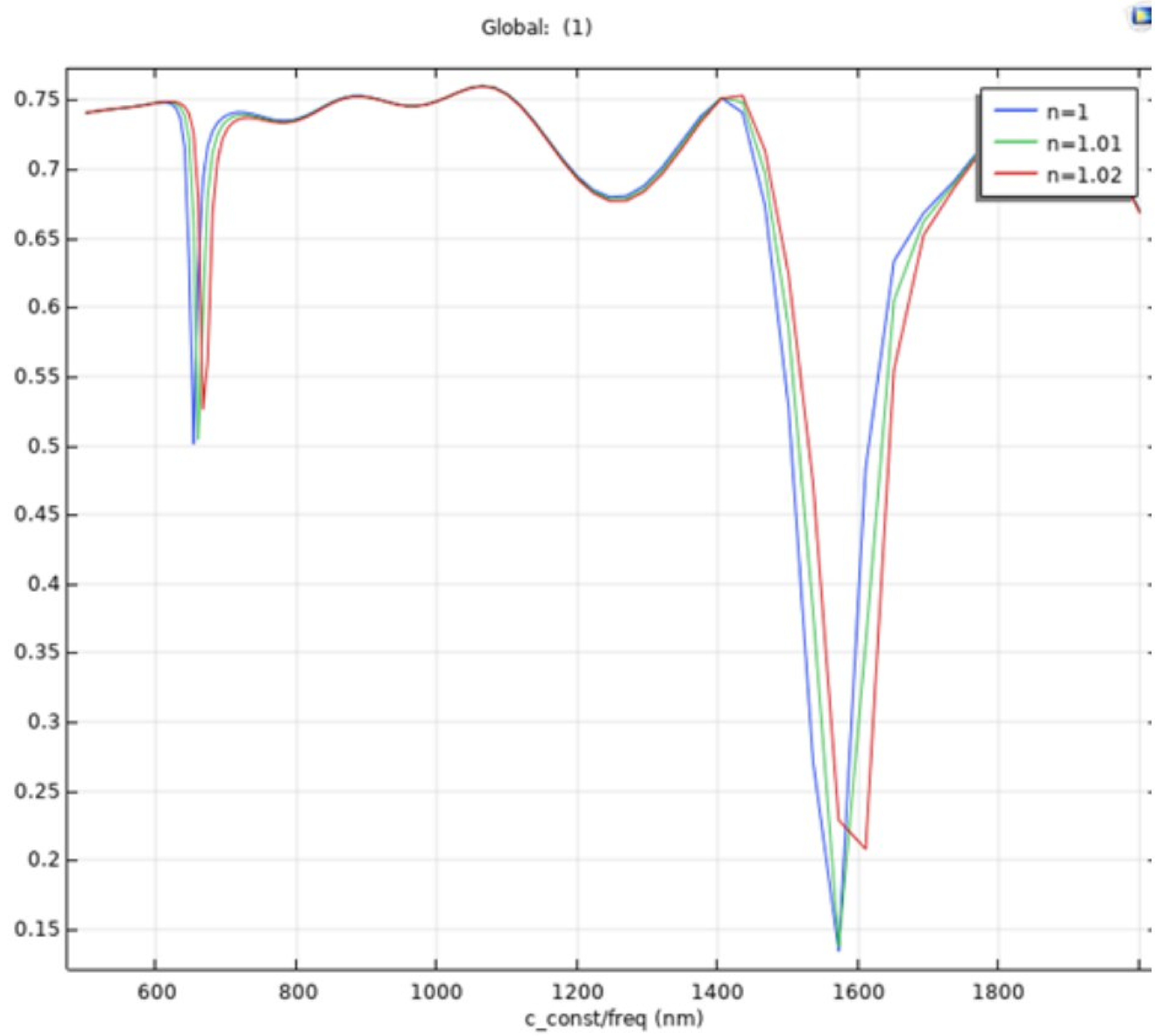

Figure 4.6 Transmittance vs Wavelength of n-Si

4.2.2 p-Si

Group III elements can dope silicon p-type. Because electrons that work on the conduction in silicon have a substantially smaller effective mass than holes, the plasma frequency for n-type silicon will be larger than for p-type silicon at the same doping amount. Group III elements can dope silicon p-type. The plasma frequency for n-type silicon will be larger than for p-type silicon at the same doping amount.

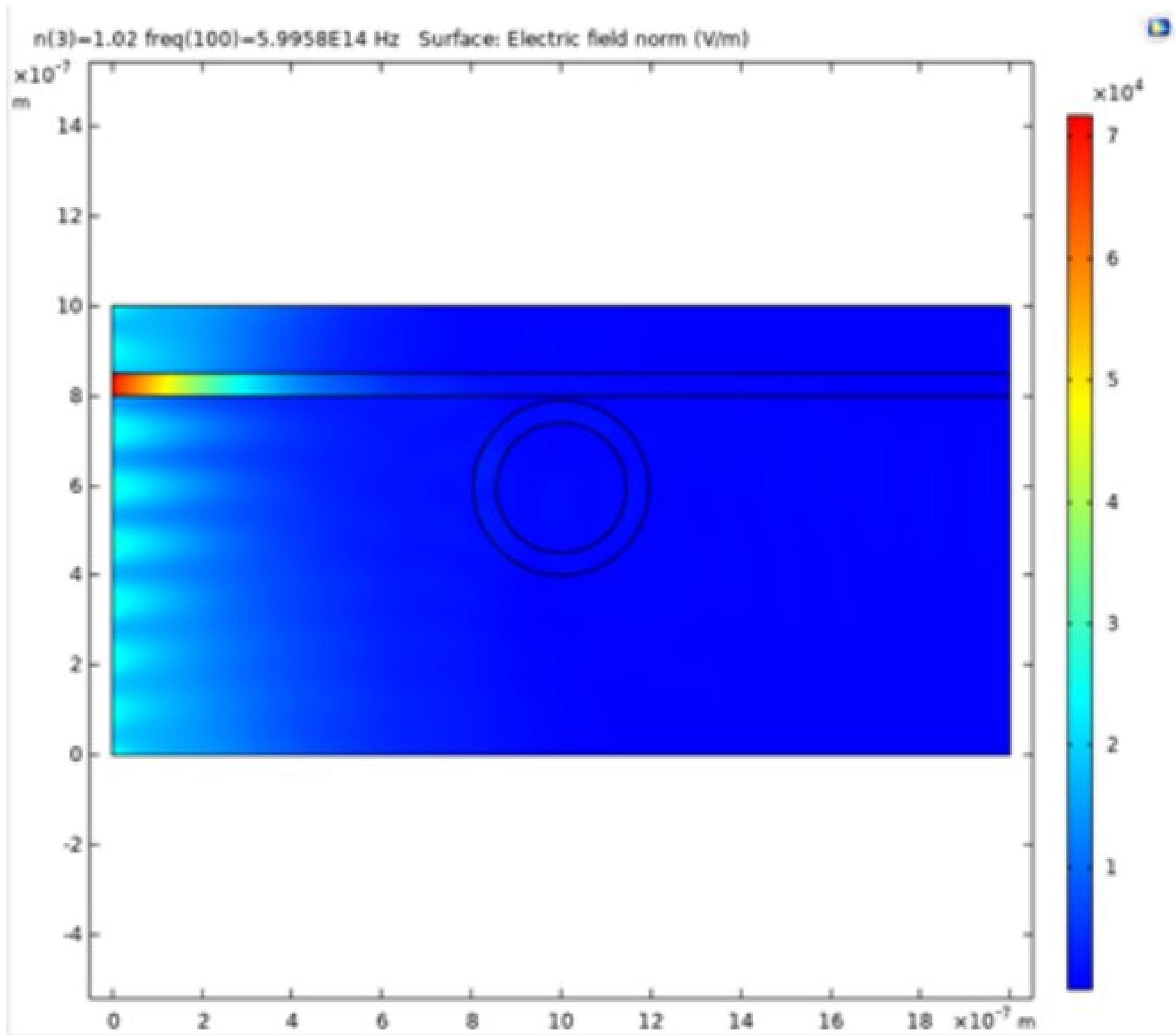

Figure 4.7 Electric Field(EWFD) of p-Si

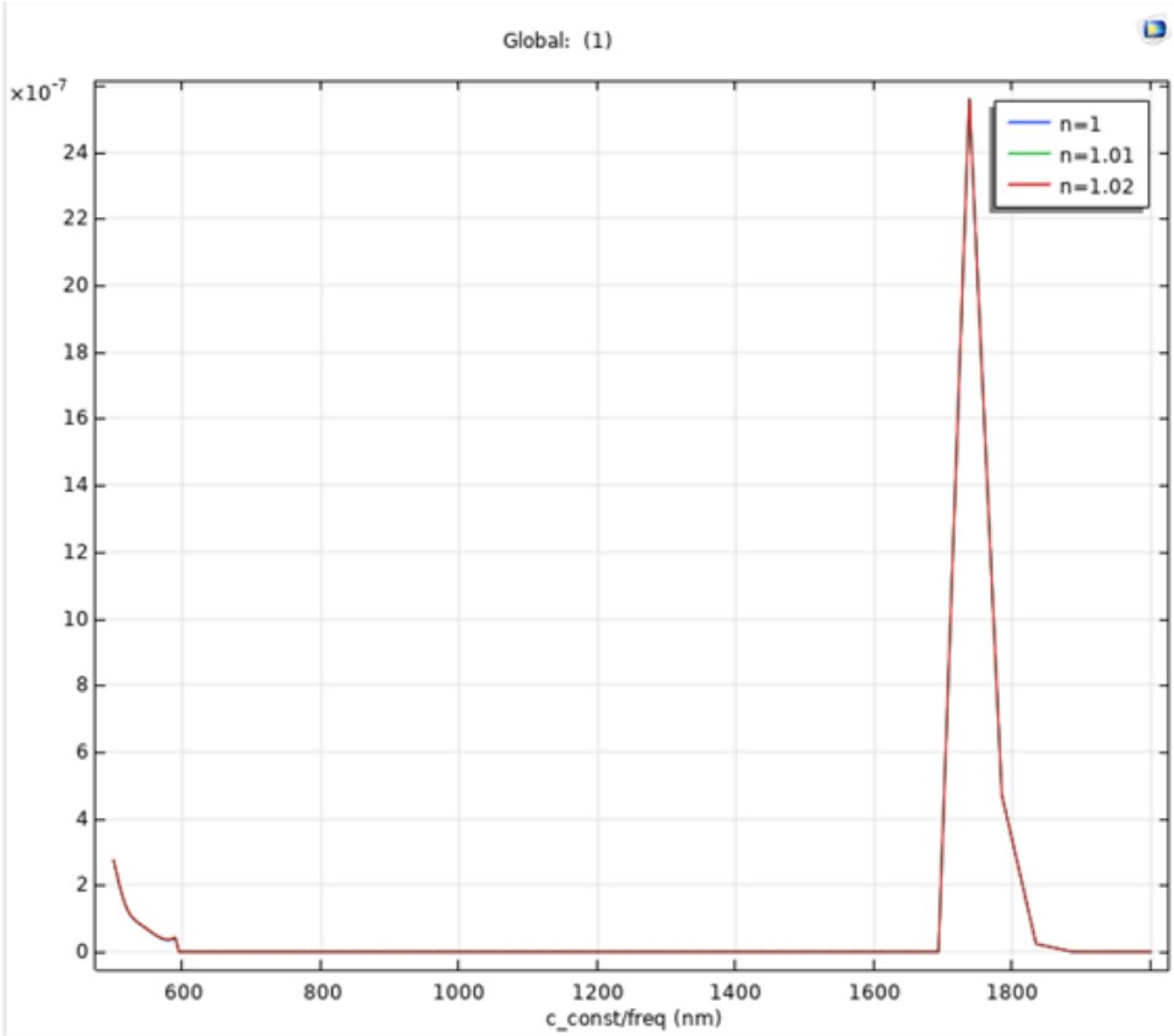

Figure 4.8 Transmittance vs Wavelength of p-Si

4.2.3 n-SiGe

In p-type nanostructured bulk silicon germanium (SiGe) alloys, a dimensionless thermoelectric figure-of-merit (ZT) of 0.95 is attained, which is around 90% higher than what is currently employed in space travel missions and 50% higher than the previous record in p-type SiGe alloys. Germanium is appealing because it has a better electron mobility and a lower optical band gap than silicon, allowing photodetectors to be made at telecommunication frequencies.

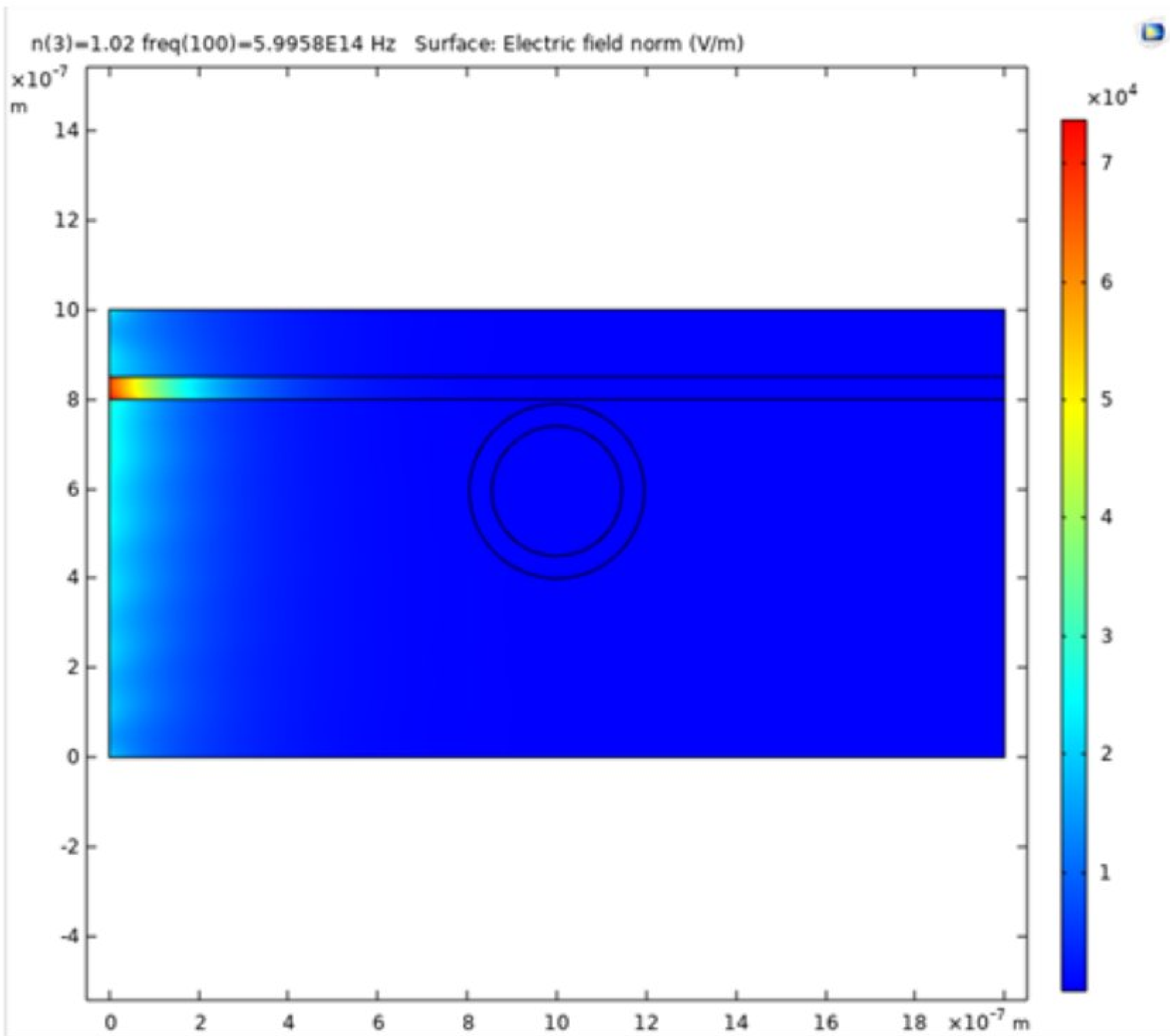

Figure 4.9 Electric Field(EWFD) of n-SiGe

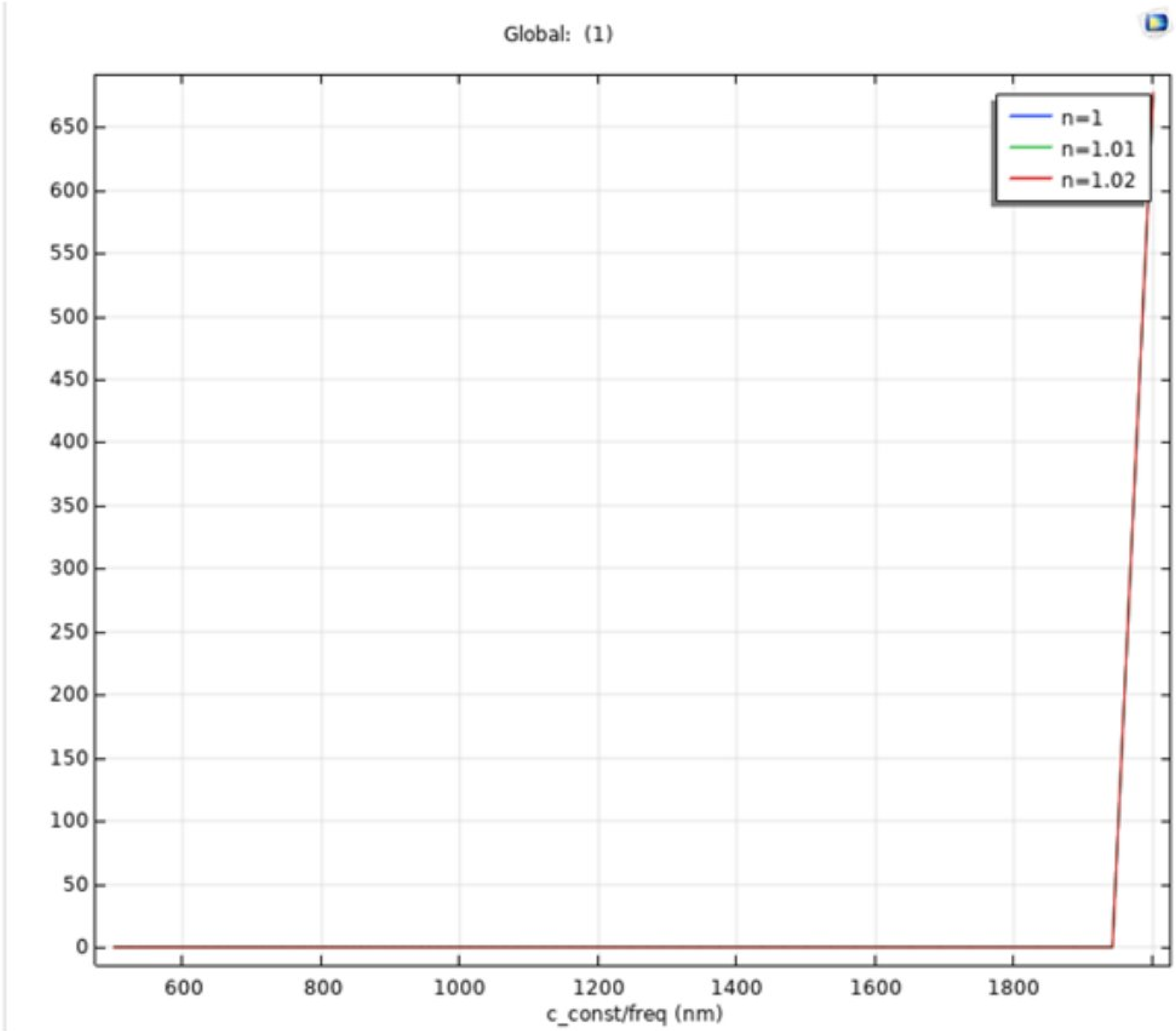

Figure 4.10 Transmittance vs Wavelength of p-SiGe

4.2.4 n-GaAs

GaAs and InP are semiconductors which have optical band gaps similar to near infrared. These semiconductors have been utilized to tune the properties of photonic devices via the electric field effect. The traditional model, which ignores mode coupling and electron-electron scattering, predicts that acoustic modes will dominate in this region.

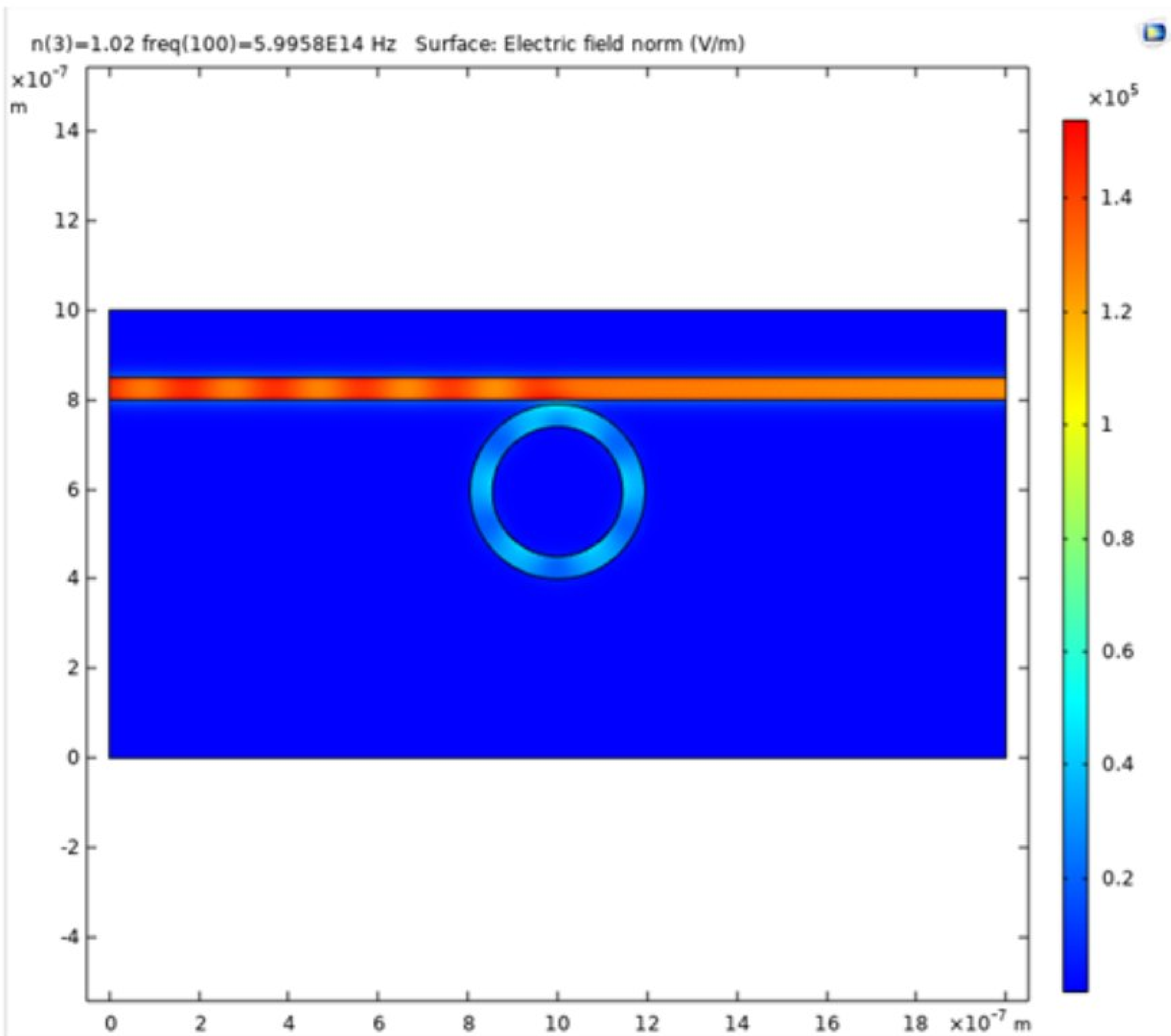

Figure 4.11 Electric Field(EWFD) of n-GaAs

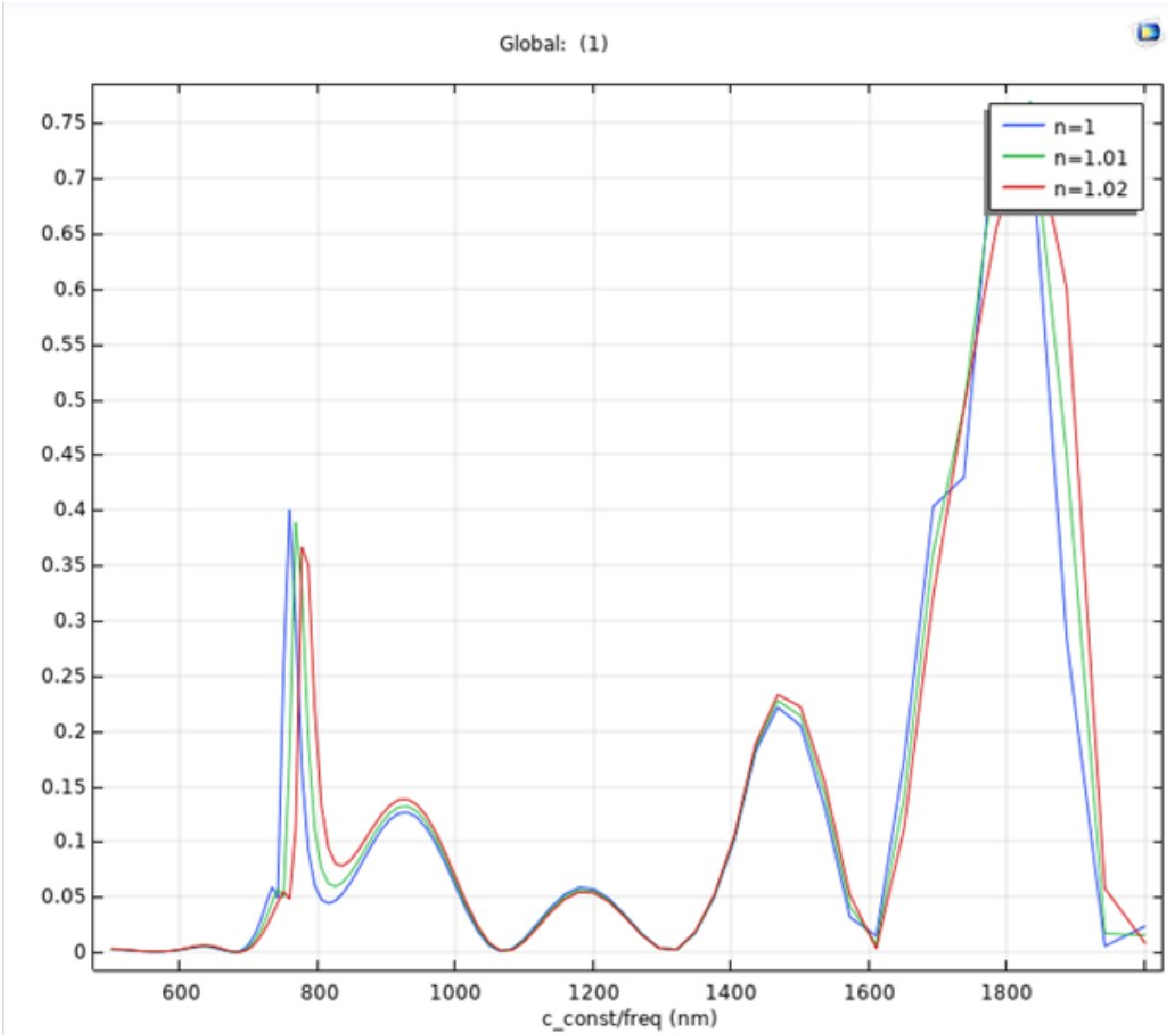

Figure 4.12 Transmittance vs Wavelength of n-GaAs

4.2.5 p-GaAs

The lattice vibrations and peculiarities coupling in GaAs are investigated by a dielectric function which is based on the model of arbitrary bonded oscillators. For heavily doped p-GaAs, the hole-plasmon characteristics we obtain produce an infrared mobility that is in good agreement with the dc mobility.

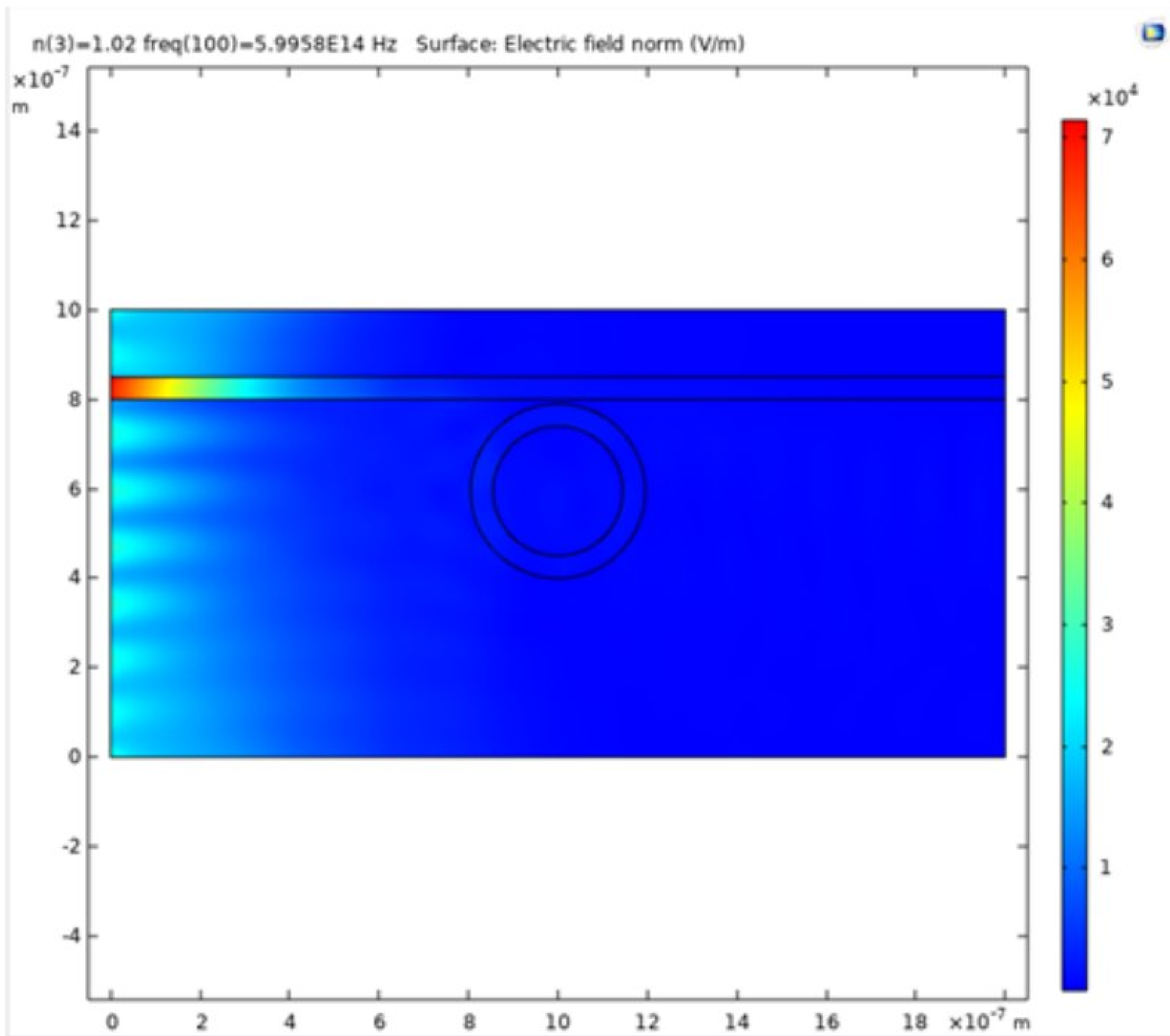

Figure 4.13 Electric Field(EWFD) of p-GaAs

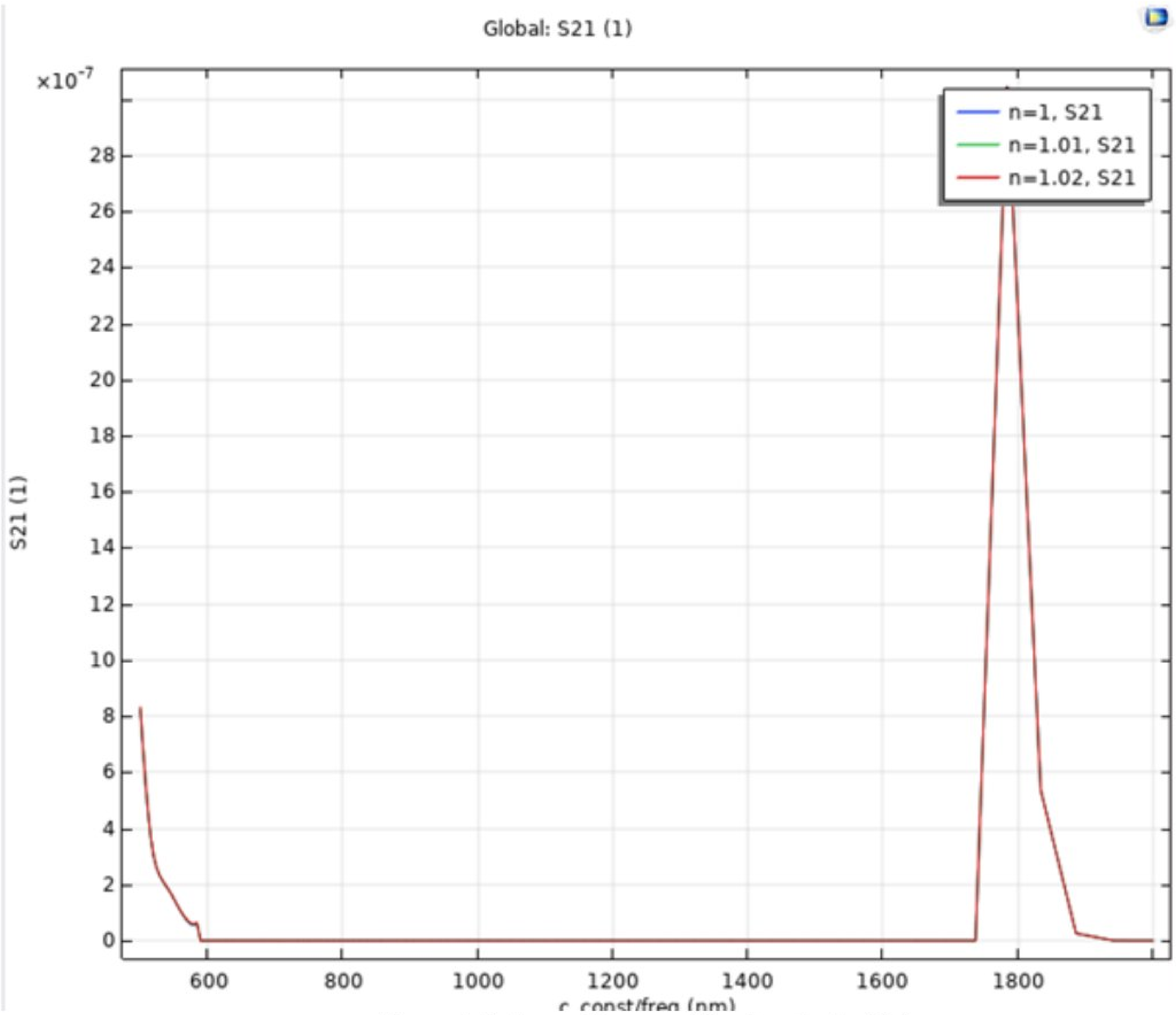

Figure 4.14 Transmittance vs Wavelength of p-GaAs

4.2.6 n-InP

At an optical communication wavelength, a multimode interference (MMI) power splitter is used. This uses an InP based waveguide which is a hybrid plasmonic. A shallow-etched conventional waveguide if an ultracompact shallow to deep transition and a waveguide of hybrid plasmonic on an InP-substrate is also presented in this study.

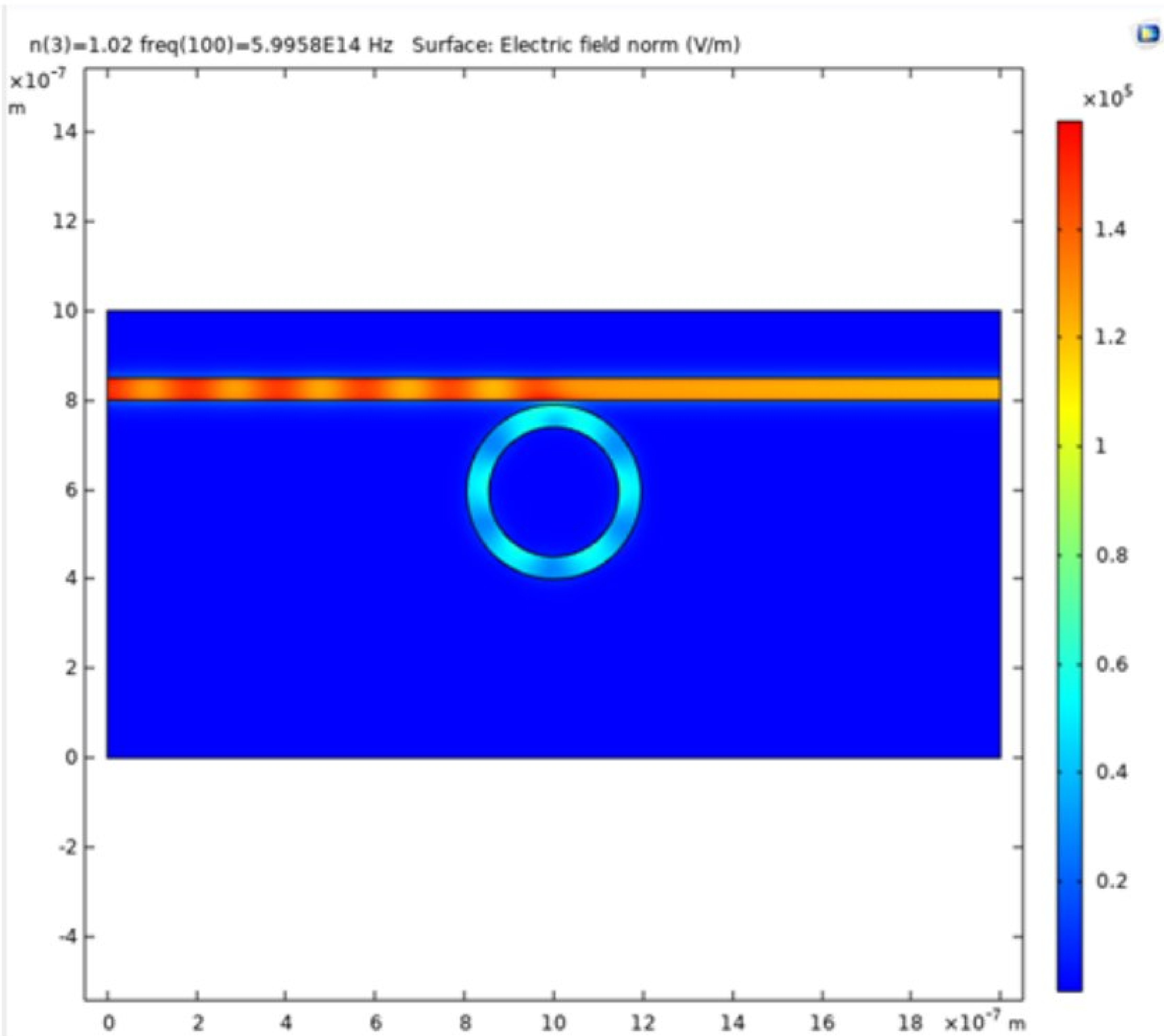

Figure 4.15 Electric Field(EWFD) of n-InP

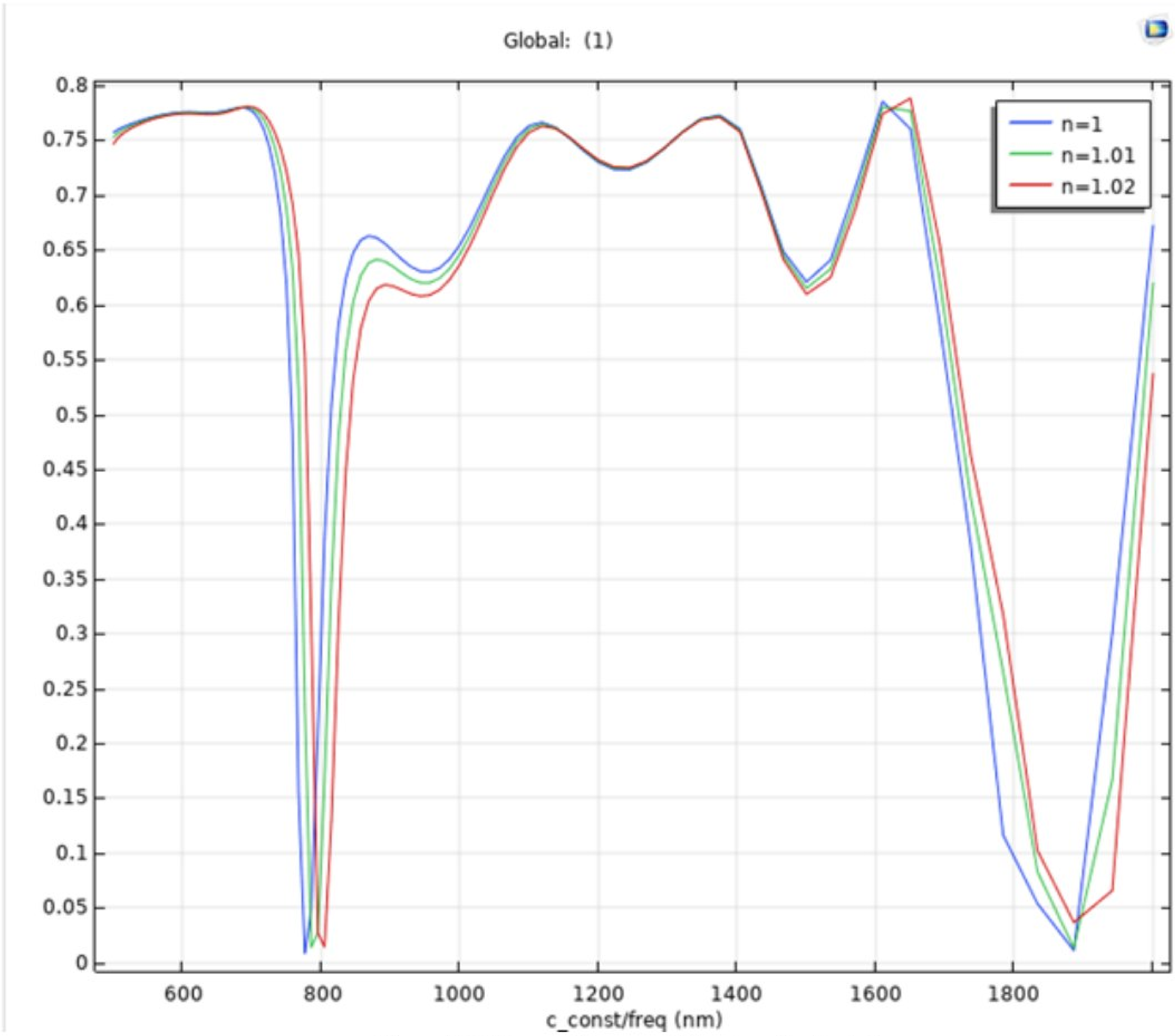

Figure 4.16 Transmittance vs Wavelength of n-InP

4.2.7 n-GaN

In LED samples with high QW-SP coupling, the photoluminescence and EL emission spectra blueshift, indicating one of the fundamental characteristics of such a coupling process. As the n-type layer has a higher carrier concentration, using the n-type side for SP generation improves performance of the device by lowering resistance and improving the QW-SP coupling effect.

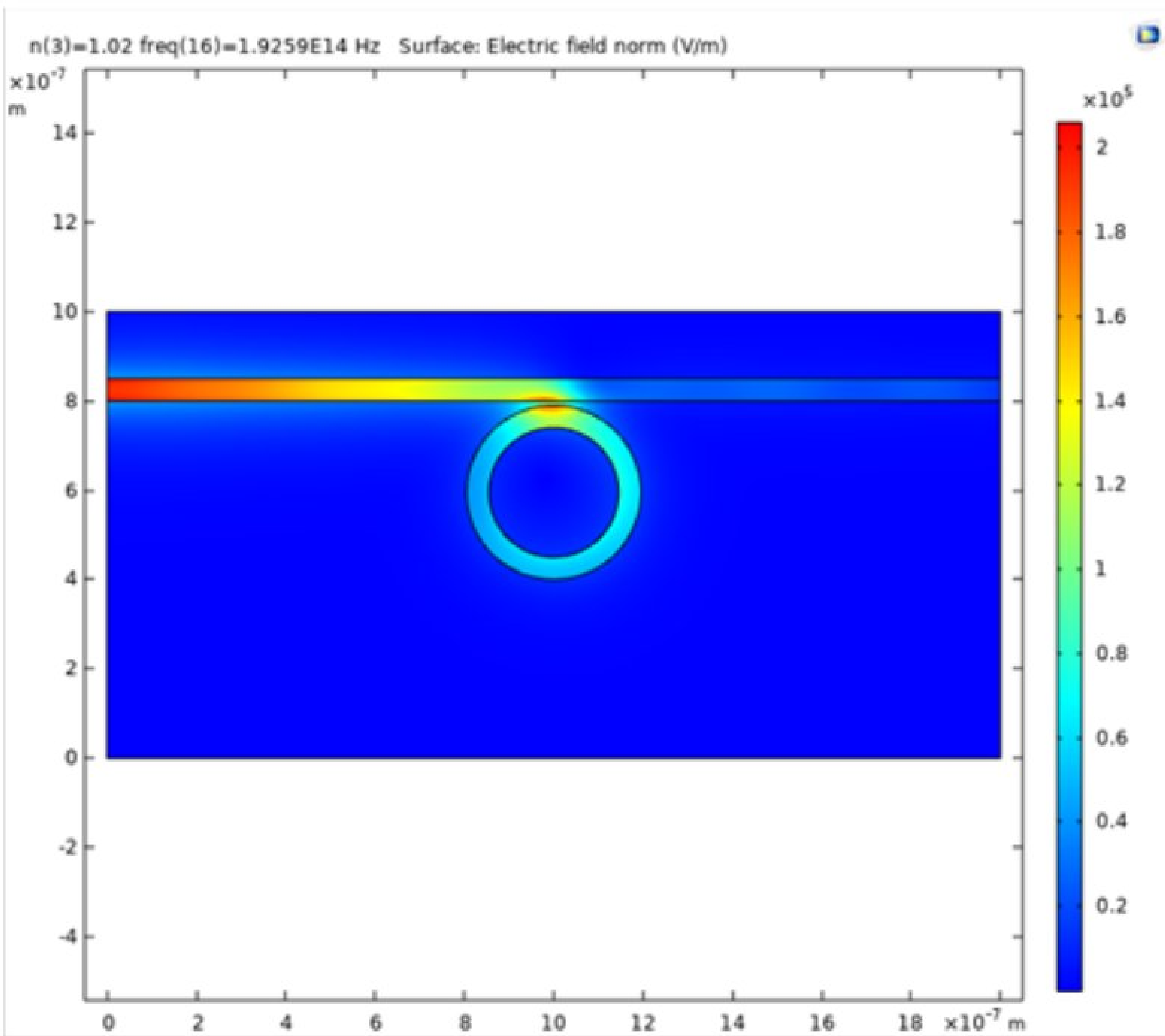

Figure 4.17 Electric Field (EWFD) of n-GaN

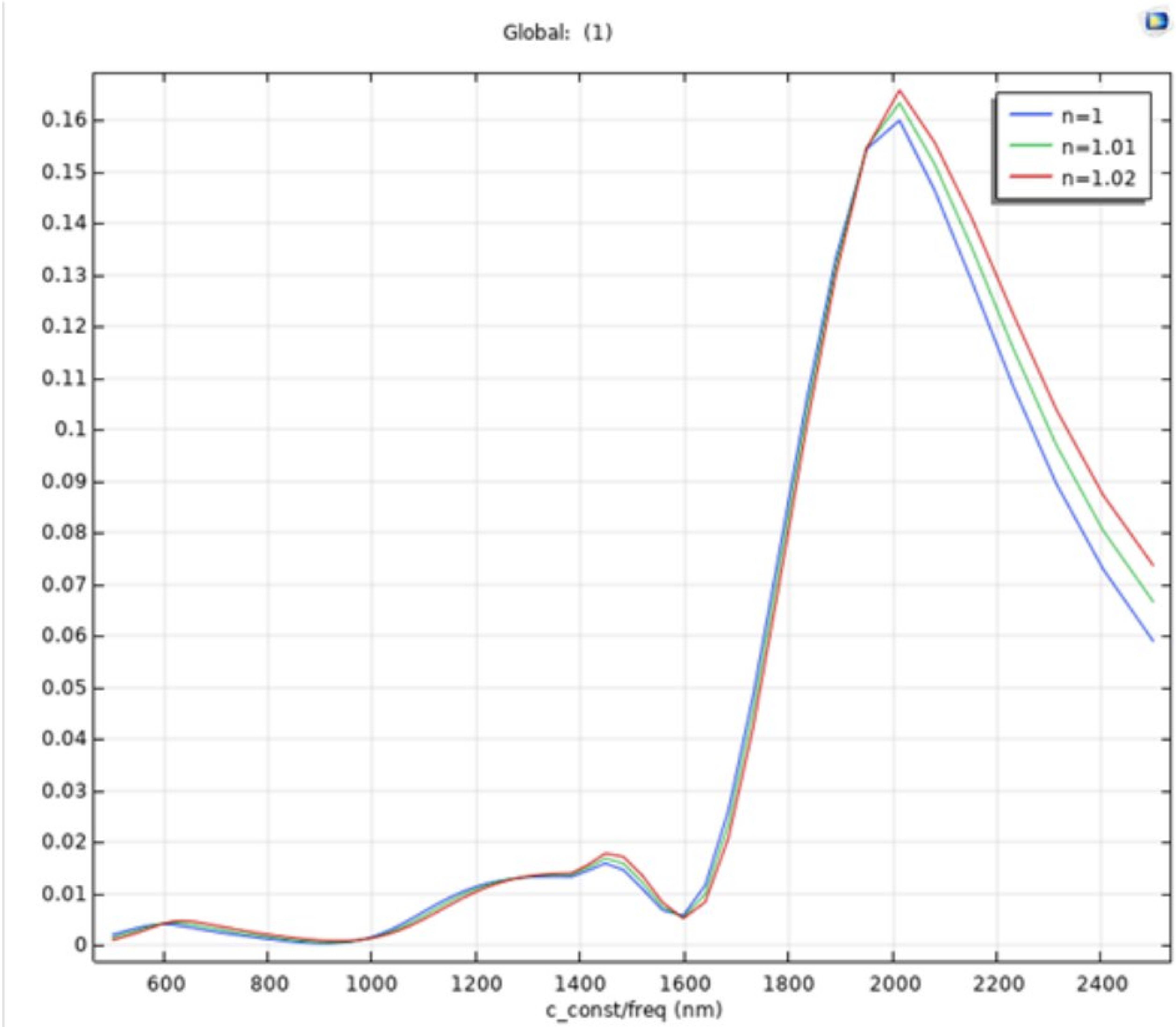

Figure 4.18 Transmittance vs Wavelength of n-GaN

4.2.8 p-GaN

Raman scattering in p-type GaN layers by coupled LO phonon-plasmon modes has been recorded for varied hole densities up to 3 1018cm3. There were plainly visible axial and planar linked modes.

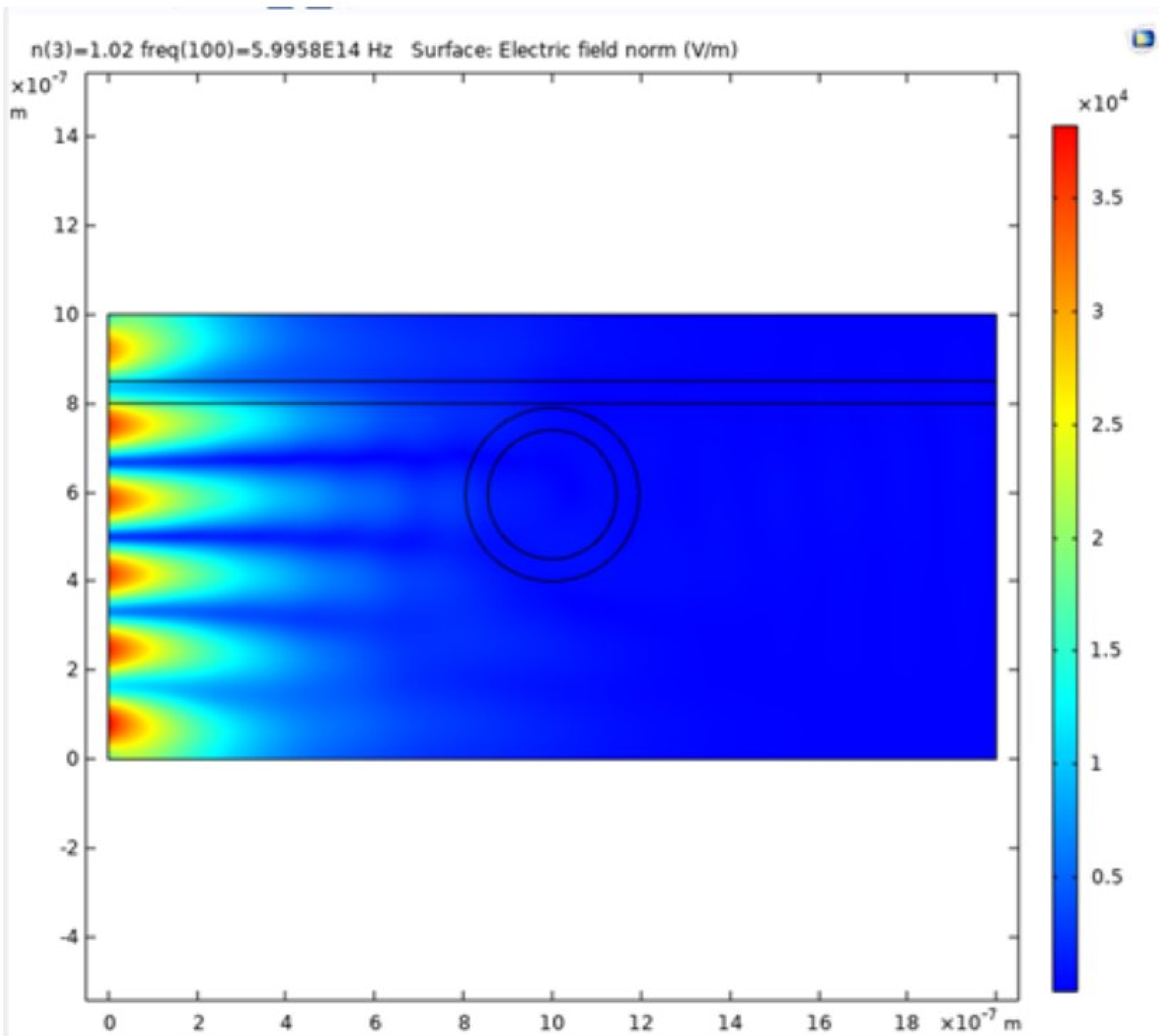

Figure 4.19 Electric Field(EWFD) of p-GaN

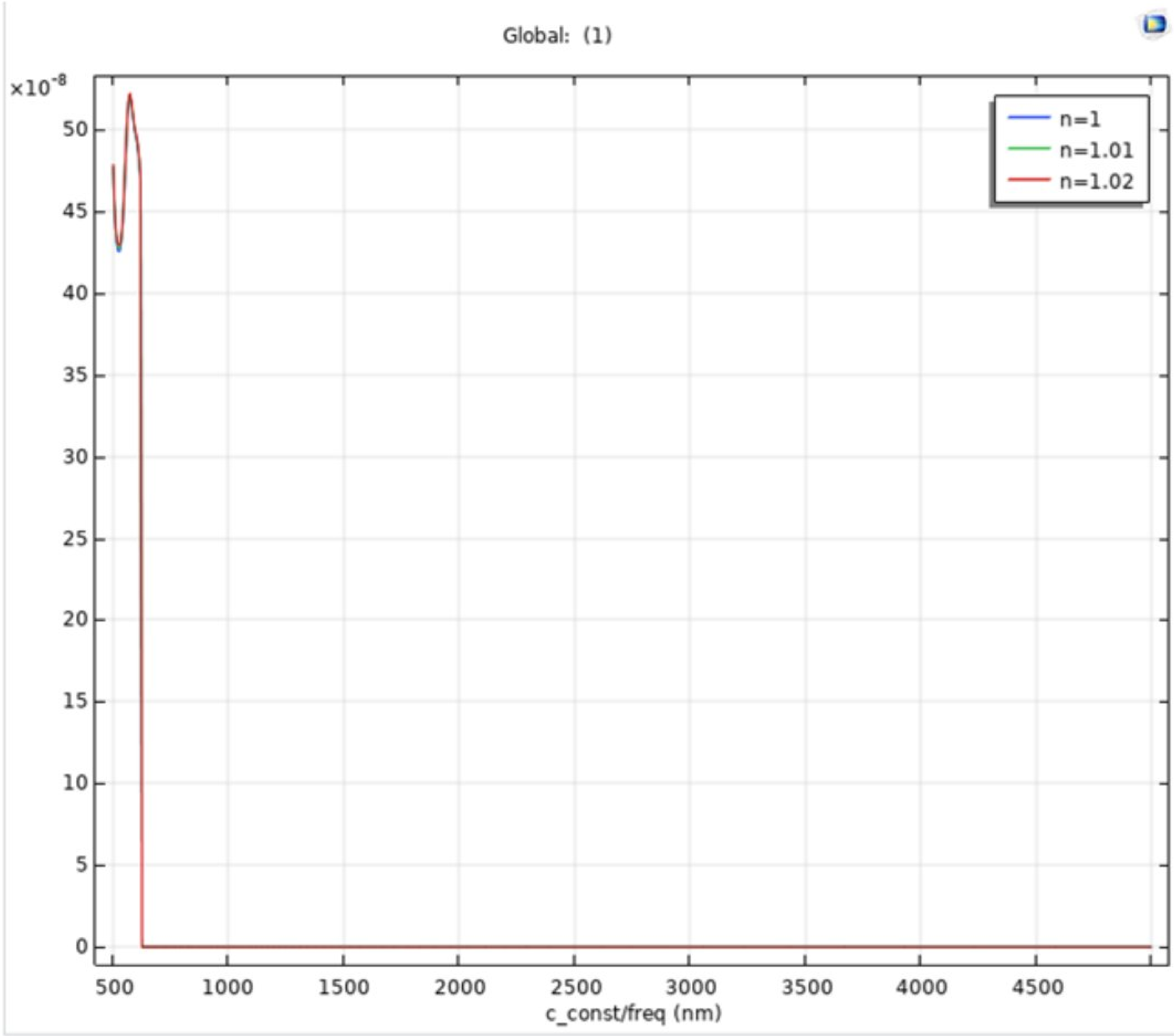

Figure 4.20 Transmittance vs Wavelength of p-GaN

4.2.9 Al:ZnO

We propose using strongly doped oxide semiconductors as an alternative to noble metals in the near-infrared wavelength region because they offer both functional and manufacturing advantages. An Al:ZnO metamaterial with a negative refraction is established. To manufacture them, conducting films are commonly used in display panels to form electrical contacts with the pixel circuitry.

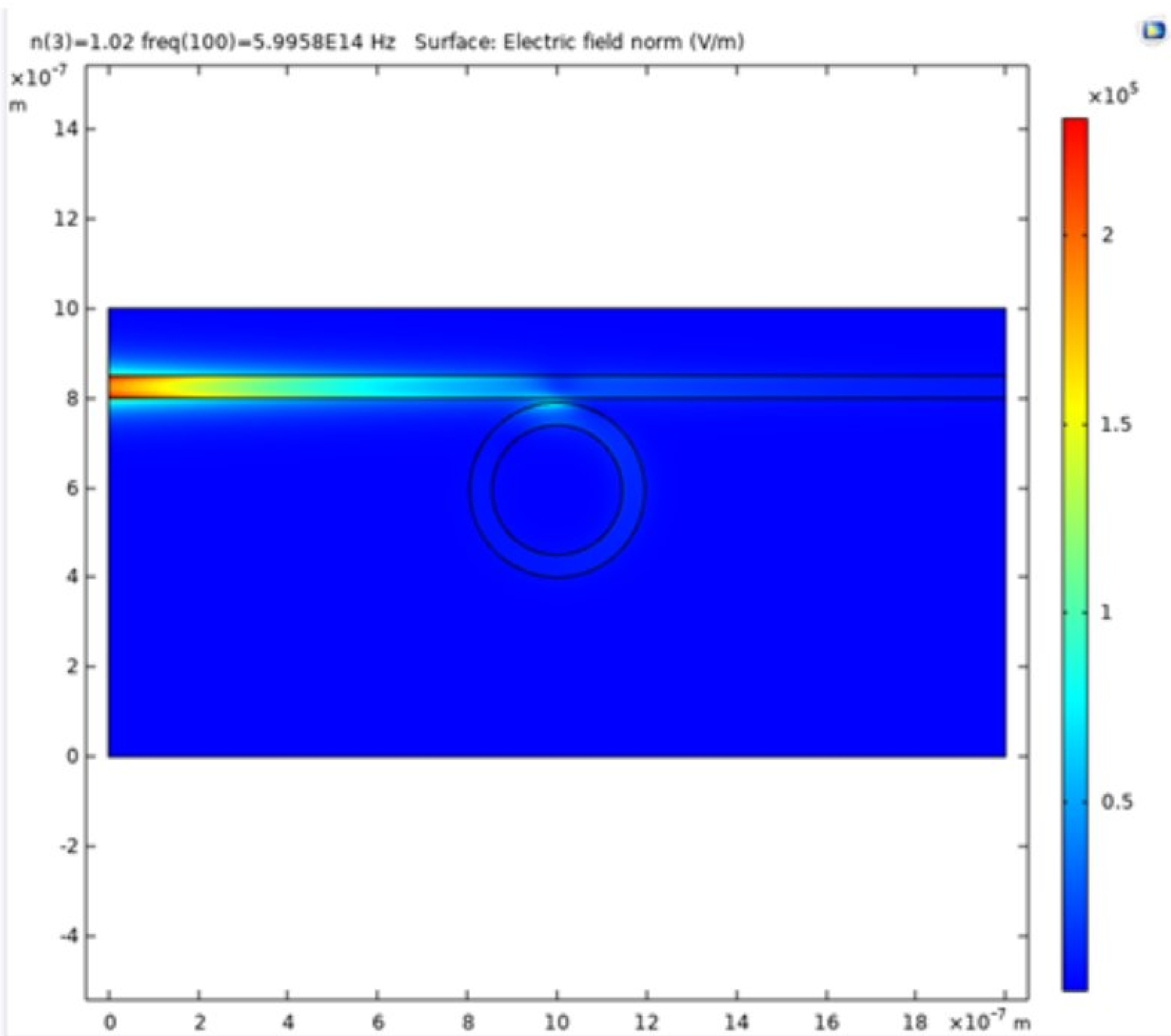

Figure 4.21 Electric Field(EWFD) of Al:ZnO

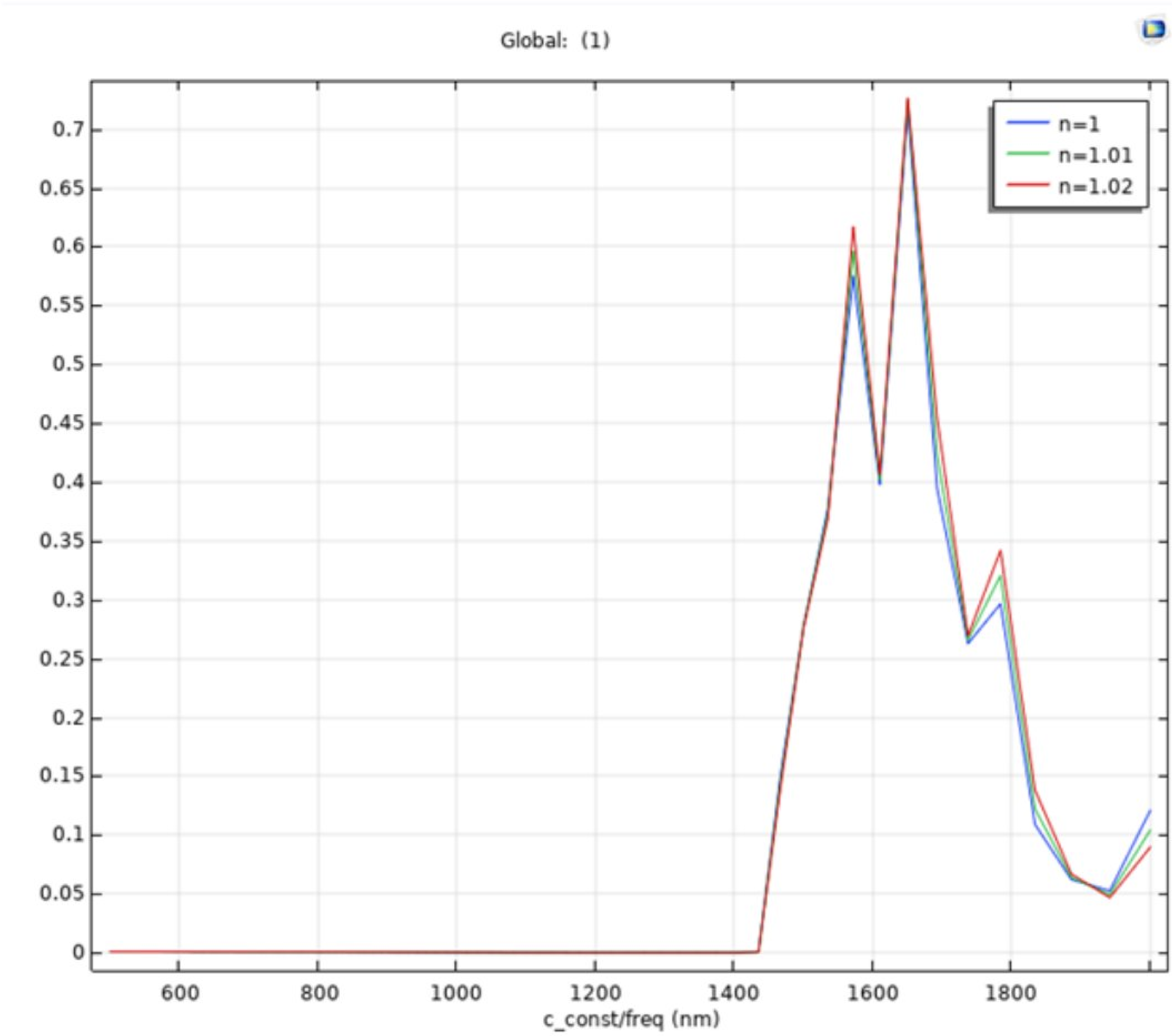

Figure 4.22 Transmittance vs Wavelength of Al:ZnO

4.2.10 Ga:ZnO

For applications in fiber-optic communication, slight adjustments in the temperature range of ZN effusion cells can result in efficient changes in Ga doping concentration. It can also show a wide range of plasmonic resonance wavelength (1400–1850 nm).

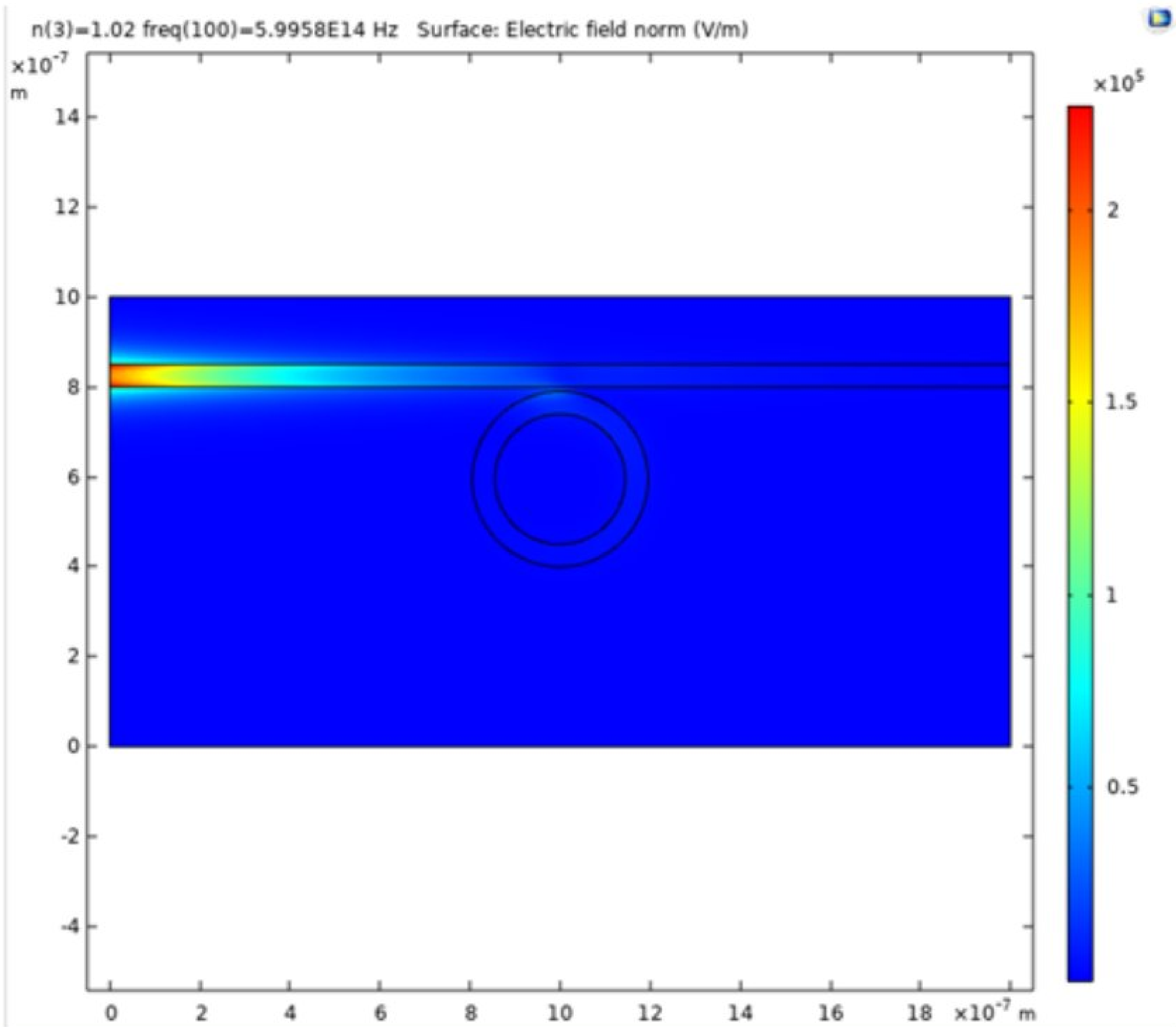

Figure 4.23 Electric Field(EWFD) of Ga:ZnO

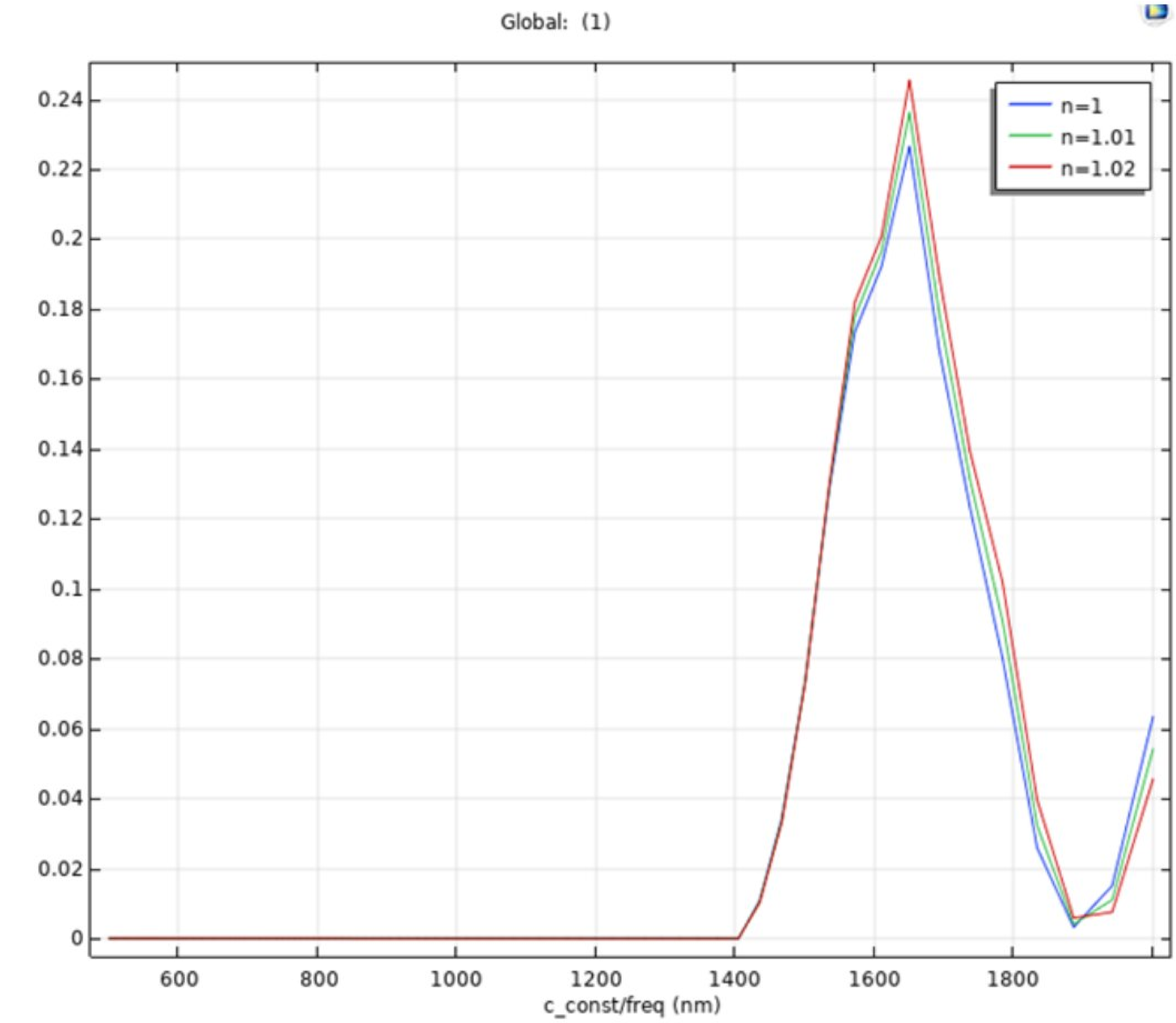

Figure 4.24 Transmittance vs Wavelength of Ga:ZnO

4.2.11 ITO

Surface plasmon dispersion curves and plasma absorption in ITO are found to be free of interband transitions, as observed in Ag but not Au. Because bound electrons contribute significantly to Au, the plasma absorption is dampened and the SPP dispersion curve is broadened. Ag is more like a free-electron conductor than Au, yet it still absorbs in the frequency range above the surface plasmon. ITO is a free-electron conductor that is virtually perfect.

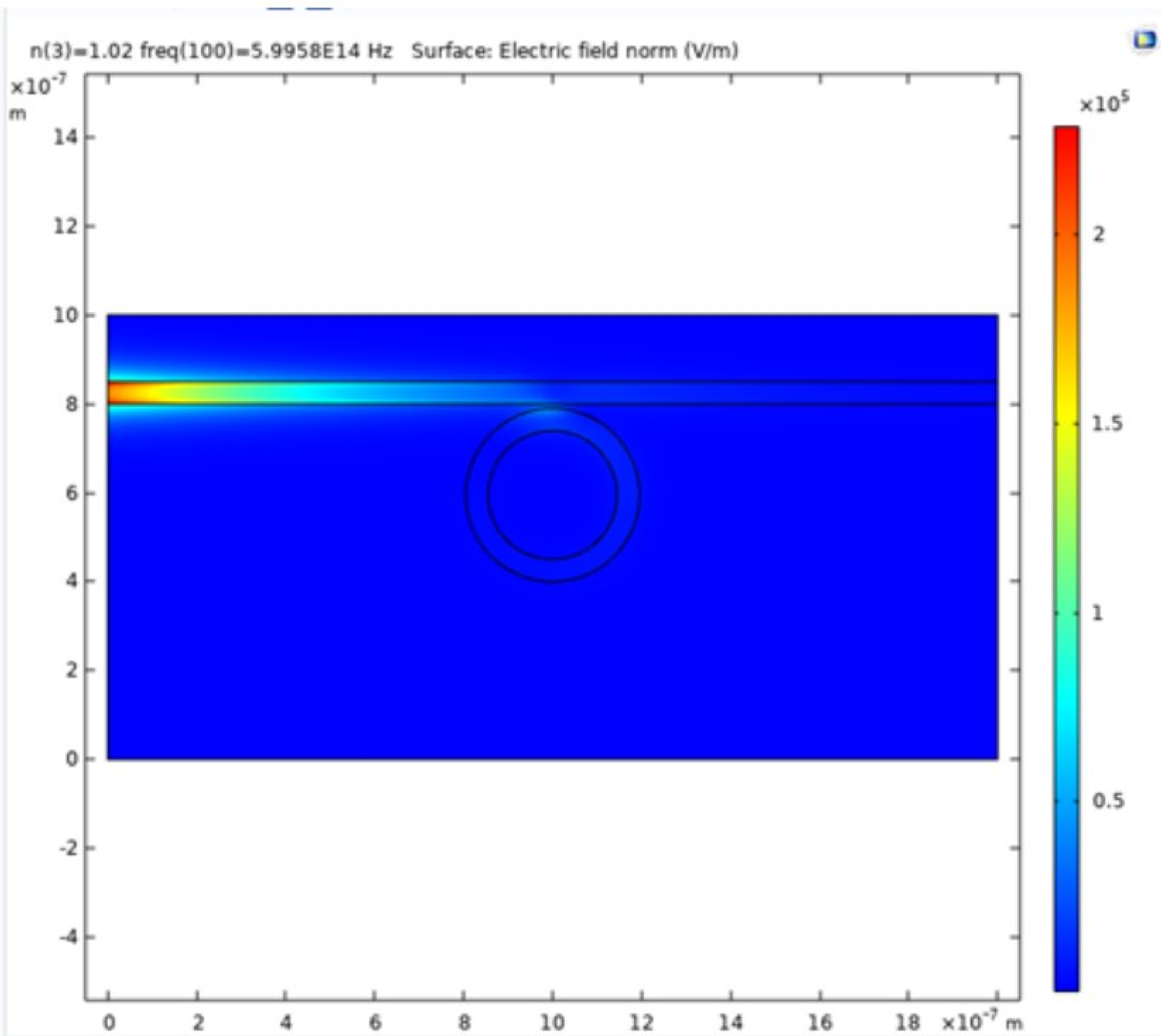

Figure 4.25 Electric Field(EWFD) of ITO

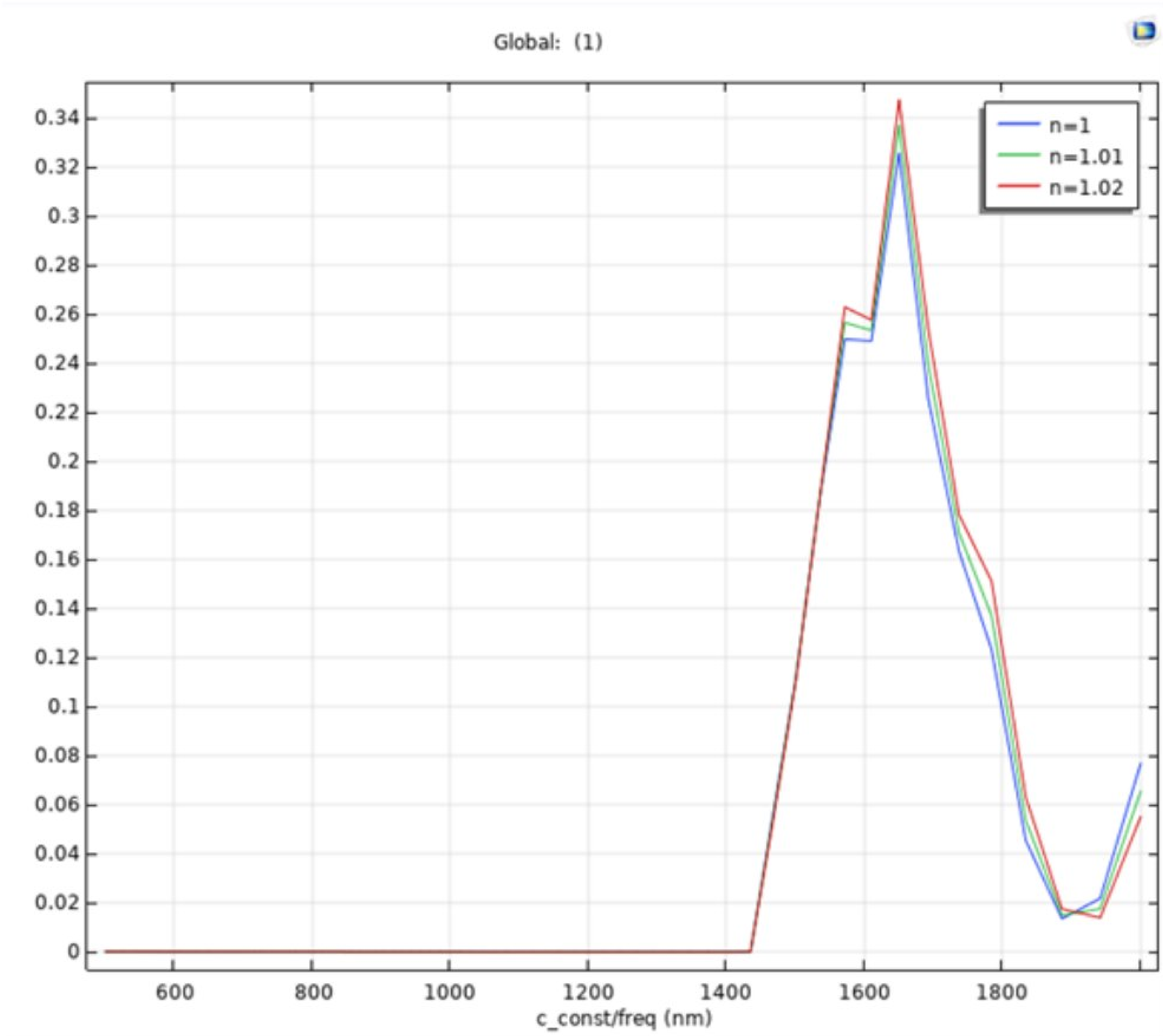

Figure 4.26 Transmittance vs Wavelength of ITO

4.2.12 Graphene

Graphene plasmonics and nonlinear optics have become intriguing new topics as a result of its rapid progress. Graphene has a two dimensional band structure. Both linear and non-linear optical capabilities have made it possible for graphene to be used in plasmonics..

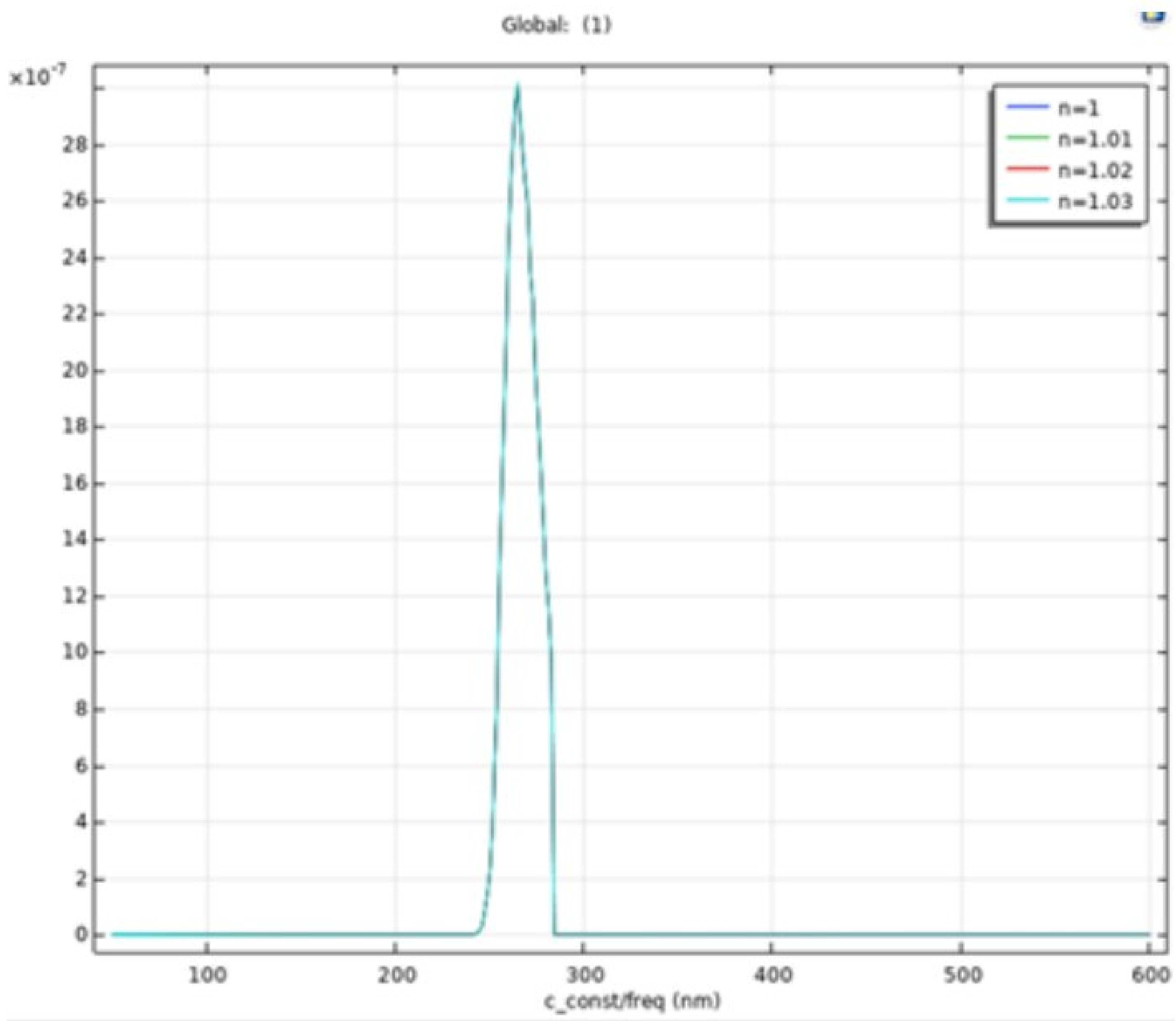

Figure 4.27 Transmittance vs Wavelength of Graphene [50-600nm]

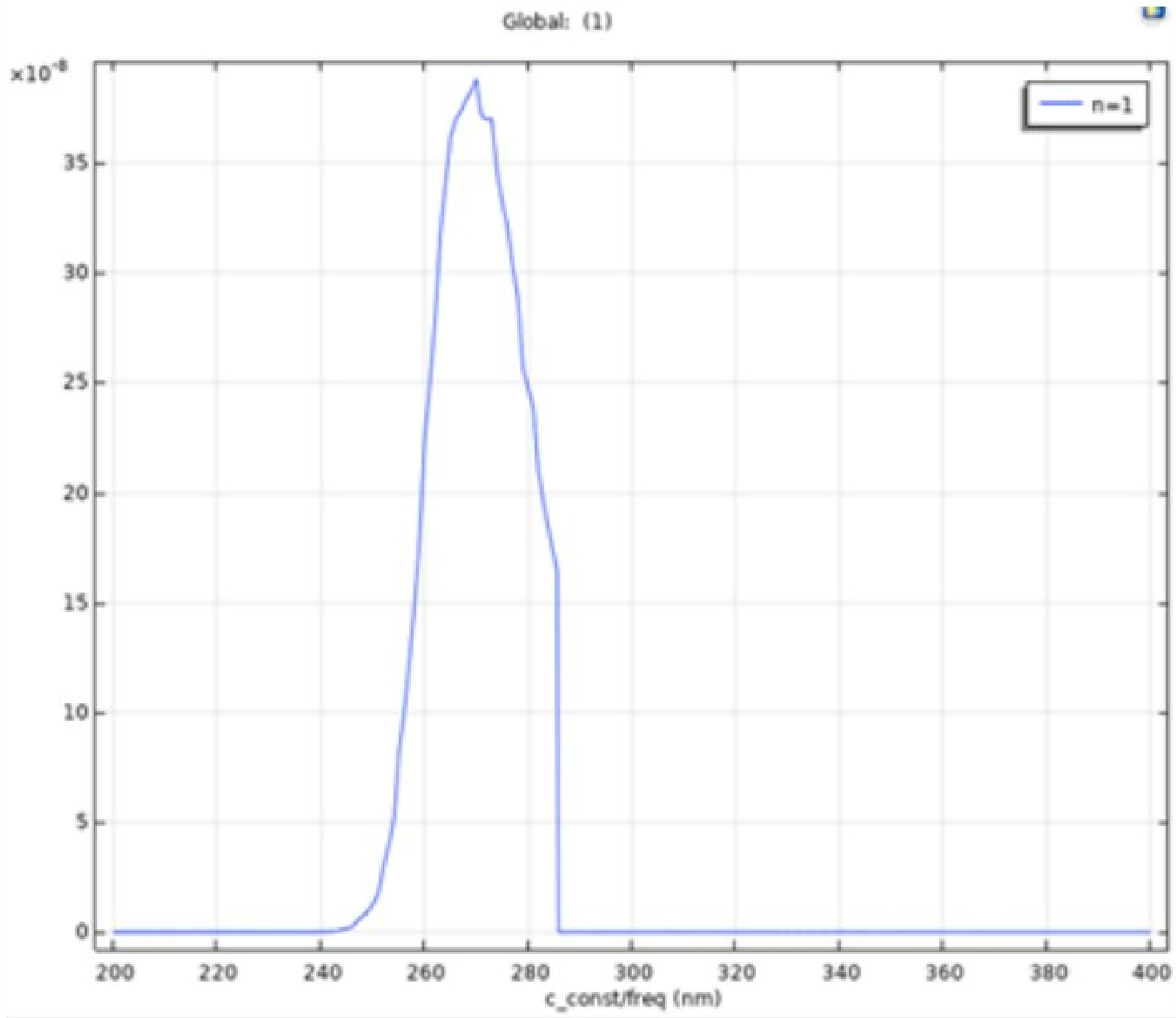

Figure 4.28 Transmittance vs Wavelength of Graphene [200-400nm]

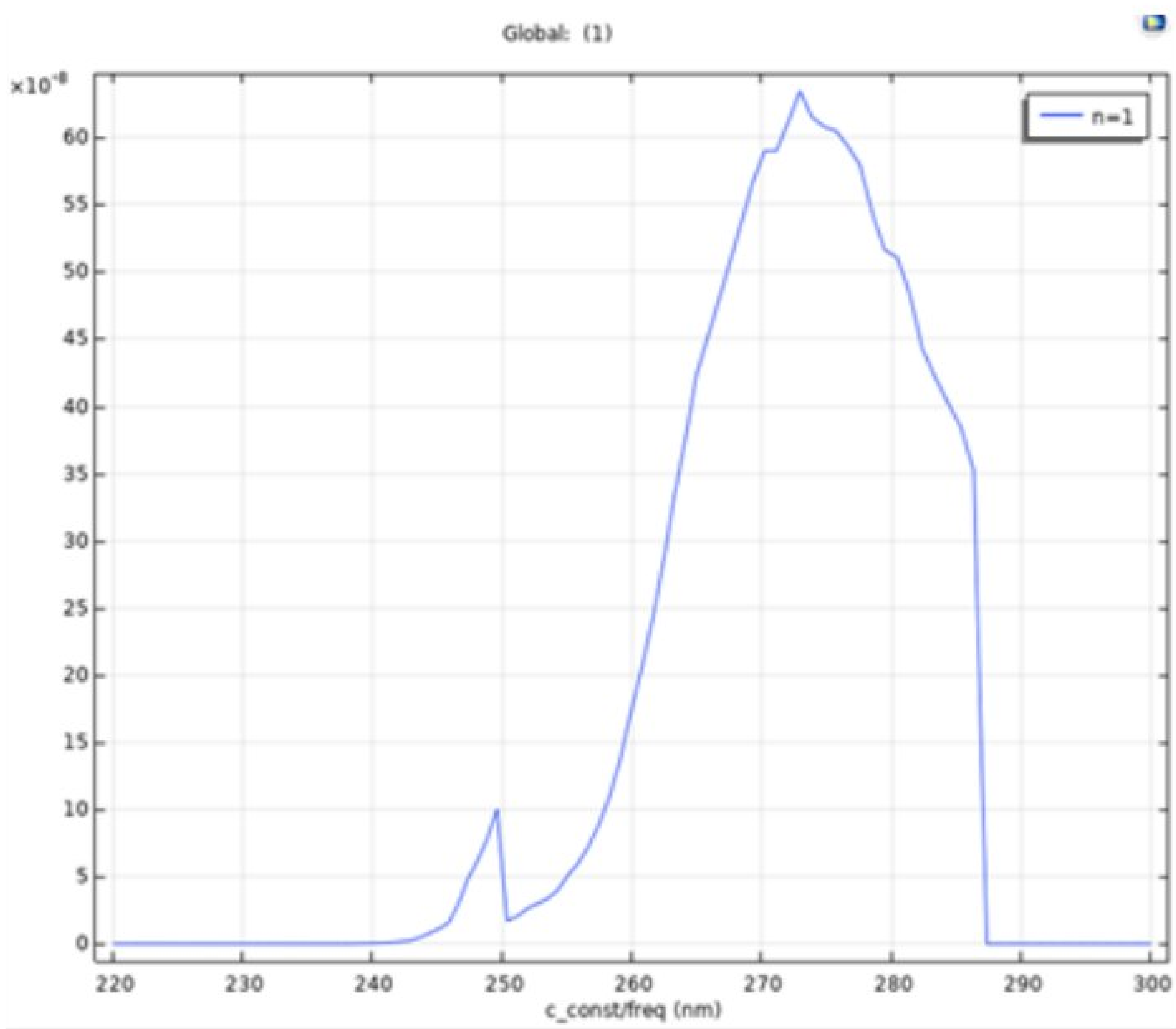

Figure 4.29 Transmittance vs Wavelength of Graphene [220-300nm]

Chapter 5

Conclusion

5.1 Comparative Analysis

From the COMSOL simulations, we generated transmittance vs wavelength graphs of different materials. For gold, we can see that from 1500-1700nm, transmittance has a crest. For silver, a few throughs at 500, 800 and 1600nm. These two materials were the reference materials for our research.

For the alternative materials, the graph of n-Si shows throughs at 650 and 1600nm. For p-Si, a crest is found at 1800nm. We did not find any crest or through for p-SiGe before 1950nm. For n-GaAs, we found some crests at 800,1600-1900nm. p-GaAs gave an almost similar graph as p-Si. For n-InP, we found some throughs at 800 and 1850nm. For n-GaN, we do not see any transmittance till 1600nm. From 1600 to 2000nm, the transmittance increases. After that, it gradually decreases. For p-GaN, we can see a crest at 600nm. After that, transmittance becomes 0.

For Al:ZnO, Ga:ZnO and ITO, the graphs are almost similar. All three materials do not have any transmittance before 1400nm. It increases till 1700nm after which the transmittance starts to decrease. We also ran the simulation for graphene for different ranges of wavelength. All three graphs have a crest at a range of 240-300nm.

5.2 Possible Replacement for Gold

From the graphs, we can see that n-GaAs has the most similar transmittance vs wavelength graph. So, we can replace gold by n-GaAs.

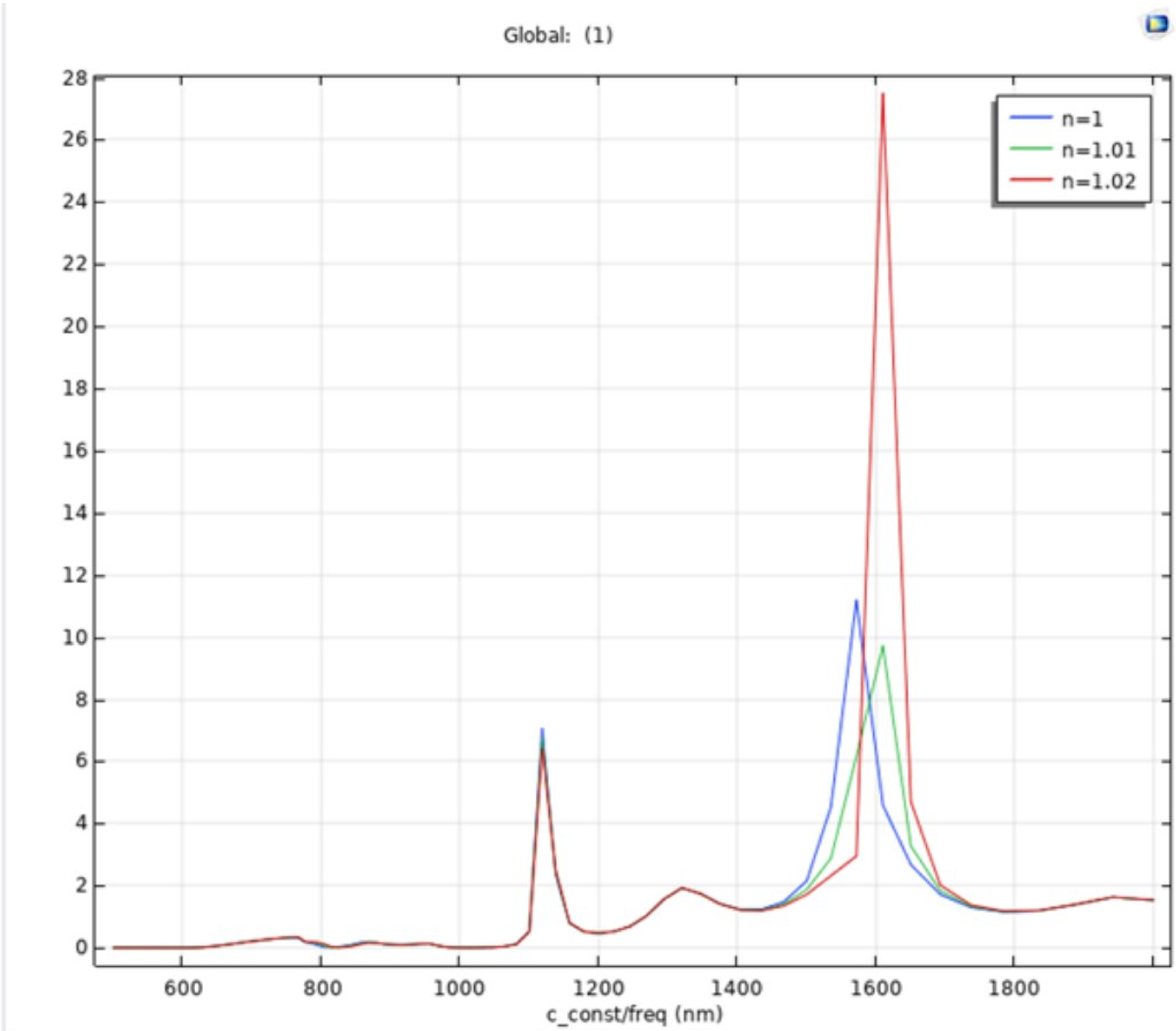

Figure 5.1 Transmittance vs Wavelength of Gold

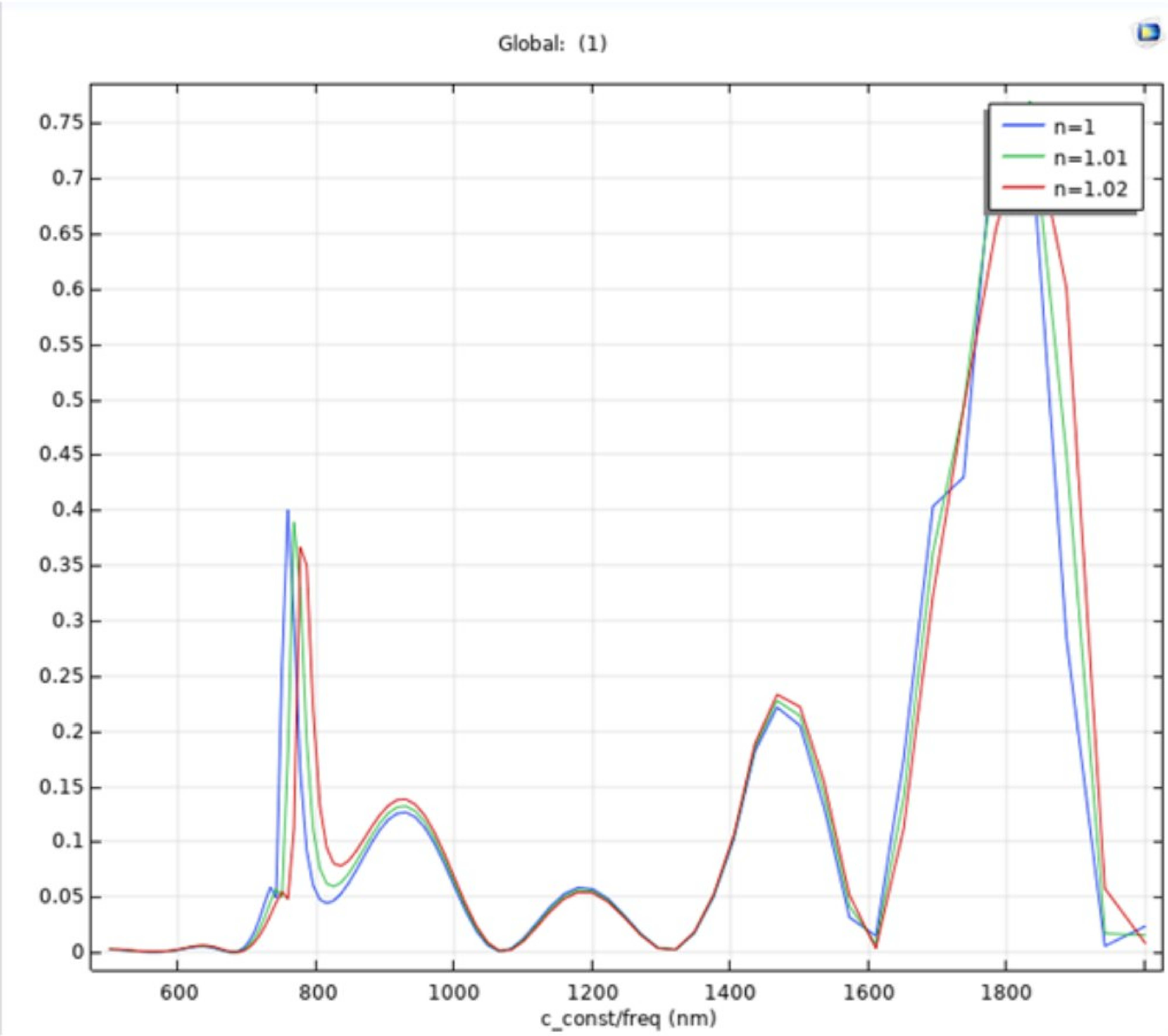

Figure 5.2 Transmittance vs Wavelength of n-GaAs

5.3 Possible Replacement for Silver

From the graphs, we can see that n-Si and n-InP have the most similar transmittance vs wavelength graph. So, we can replace silver by n-Si or n-InP.

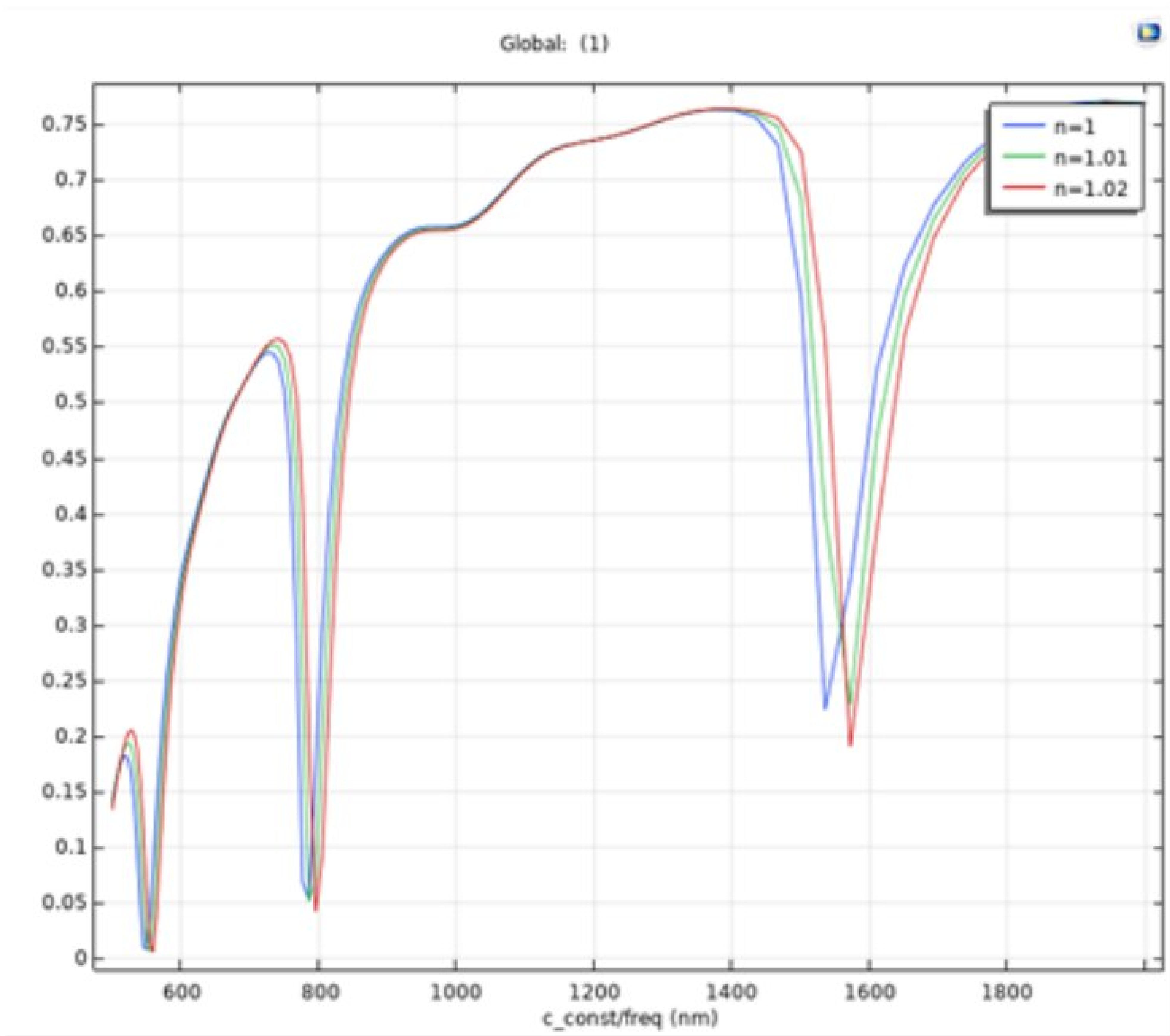

Figure 5.3 Transmittance vs Wavelength of Silver

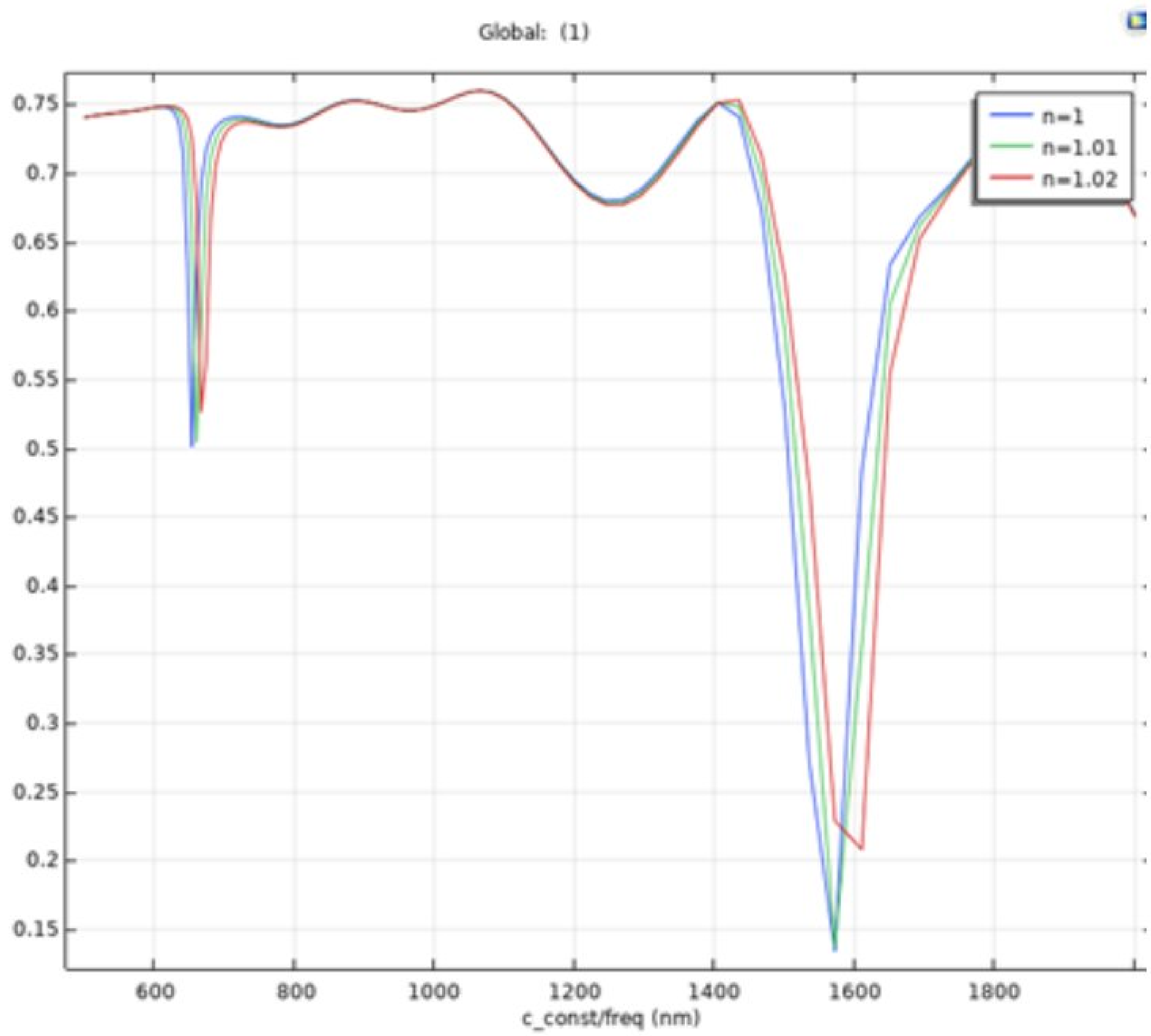

Figure 5.4 Transmittance vs Wavelength of n-Si

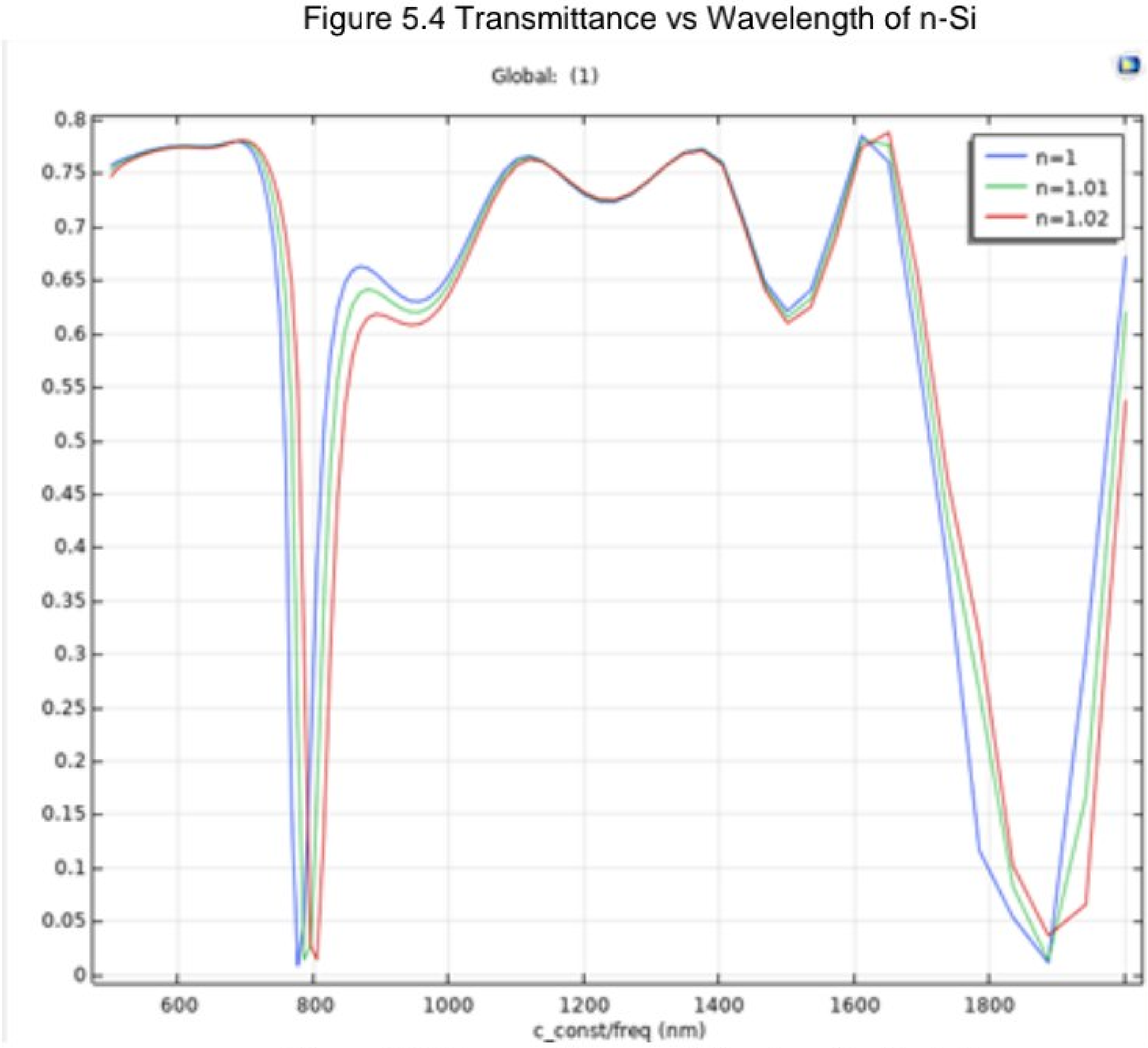

Figure 5.5 Transmittance vs Wavelength of n-InP

5.4 Summary

In order to replace gold and silver as plasmonic materials, we simulated different materials in a model generated in COMSOL. Among these materials, n-GaAs has the closest similarity with gold. Although the transmittance is lower in n-GaAs, it can be improved by changing the concentration of the doping material. As for the replacement for silver, we found n-Si and n-InP as replacements because both of them have almost the same transmittance vs wavelength graph.

References

[1] M. L. Brongersma , V. M. Shalaev , Science 2010 , 328 , 440 .
[2] P. B. Johnson , R. Christy , Phys. Rev. B 1972 , 6 , 4370 .
[3] J. Khurgin , G. Sun , Appl. Phys. Lett. 2010 , 96 , 181102 .
[4] M. Balkanski , A. Aziza , E. Amzallag , Physica Status Solidi B 1969 , 31 , 323 .
[5] D. Schroder , R. N. Thomas , J. C. Swartz , IEEE J. Solid-State Circuits 1978 , 13 , 180 .
[6] G. Kroesen , G. Oehrlein , E. De Frésart , G. Scilla , Appl. Phys. Lett. 1992 , 60 , 1351 .
[7] W. Walukiewicz , L. Lagowski , L. Jastrzebski , M. Lichtensteiger , H. C. Gatos , J. Appl. Phys. 1979 , 50 , 899 .
[8] T. Yamada , E. Tokumitsu , K. Saito , T. Akatsuka , M. Miyauchi , M. Konagai , K. Takahashi , J. Cryst. Growth 1989 , 95 , 145 .
[9] W. Walukiewicz , J. Lagowski , L. Jastrzebski , P. Rava , M. Lichtensteiger , C. H. Gatos , H. C. Gatos , J. Appl. Phys. 1980 , 51 , 2659 .
[10] A. Kasic , M. Schubert , S. Einfeldt , D. Hommel , T. Tiwald , Phys. Rev. B 2000 , 62 , 7365 .
[11] H. Agura , A. Suzuki , T. Matsushita , T. Aoki , M. Okuda , Thin Solid Films 2003 , 445 , 263 .
[12] S. M. Park , T. Ikegami , K. Ebihara , Thin Solid Films 2006 , 513 , 90 .
[13] S. Ray , R. Banerjee , N. Basu , A. Batabyal , A. Barua , J. Appl. Phys. 1983 , 54 , 3497 .
[14] G. Backenstoss , Phys. Rev. 1957 , 108 , 1416 .
[15] J. P. Dismukes , L. Ekstrom , E. F. Steigmeier , I. Kudman , D. S. Beers , J. Appl. Phys. 1964 , 35 , 2899 .
[16] D. Szmyd , M. Hanna , A. Majerfeld , J. Appl. Phys. 1990 , 68 , 2376 .
[17] F. Kesamanly , Y. V. Maltsev , D. Nasledov , Y. I. Ukhanov , Phys. Status Solidi B 1966 , 13 , K119 .
[18] F. Trumbore , Bell Syst. Tech. J 1960 , 39 , 205 .
[19] J. Neave , P. Dobson , J. Harris , P. Dawson , B. Joyce , Appl. Phys. A: Mater. Sci. Process. 1983 , 32 , 195 .
[20] P. Hageman , W. Schaff , J. Janinski , Z. Liliental-Weber , J. Cryst. Growth 2004 , 267 , 123 .
[21] G. V. Naik , J. Kim , A. Boltasseva , Opt. Mater. Express 2011 , 1 , 1090 .
[22] J. Kim , G. V. Naik , N. K. Emani , U. Guler , A. Boltasseva , IEEE J. Sel. Top. Quantum Electron. 2013 , DOI: 10.1109/jstqe.2013.2238611.
[23] C. Rhodes , S. Franzen , J. P. Maria , M. Losego , D. N. Leonard , B. Laughlin , G. Duscher , S. Weibel , J. Appl. Phys. 2006 , 100 , 054905 .
[24] P. R. West , S. Ishii , G. V. Naik , N. K. Emani , V. M. Shalaev , A. Boltasseva , Laser Photonics Rev. 2010 , 4 , 795 .
[25] P. Drude , Ann. Phys. 1900 , 306 , 566 .
[26] N. W. Ashcroft , N. D. Mermin , Solid State Physics , Saunders College , Philadelphia, PA, USA 1976 .

[27] J. S. G. Bouillard , W. Dickson , D. P. O'Connor , G. A. Wurtz , A. Zayats , Nano Lett. 2012
.
[28] W. Cai , U. K. Chettiar , A. V. Kildishev , V. M. Shalaev , Nat. Photonics 2007 , 1 , 224 .
[29] R. Cohen , G. Cody , M. Coutts , B. Abeles , Phys. Rev. B 1973 , 8 , 3689 .
[30] Y. Yagil , G. Deutscher , Thin Solid Films 1987 , 152 , 465 .
[31] F. Abelès , Y. Borensztein , T. López-Rios , Advances in Solid State Physics , Vol. 24 (Ed: P. Grosse), Springer Berlin/Heidelberg Germany 1984 .
[32] O. Heavens , Rep. Prog. Phys. 1960 , 23 , 1 .
[33] L. Kazmerski , D. M. Racine , J. Appl. Phys. 1975 , 46 , 791 .
[34] P. Clegg , The Optical Constants of Thin Metallic Films Deposition by Evaporation , Proc. Phys. Soc., London, Sect. B 1952 , 65 , 774 .
[35] A. Denier van derGon , R. Tromp , M. Reuter , Thin Solid Films 1993 , 236 , 140 .
[36] K. H. Park , J. S. Ha , E. H. Lee , ETRI J. 1997 , 19 , 71 .
[37] V. Logeeswaran , M. L. Chan , Y. Bayam , M. Saif Islam , D. Horsley , X. Li , W. Wu , S. Wang , R. Williams , Appl. Phys. A: Mater. Sci. Process. 2007 , 87 , 187 .